5-2007

# EFFECTS OF IONIZING RADIATON ON DIAPHYSEAL CORTICAL BONE

Neil Travis
*Clemson University*, ntravis@clemson.edu

# EFFECTS OF IONIZING RADIATON ON DIAPHYSEAL CORTICAL BONE

---

A Thesis
Presented to
the Graduate School of
Clemson University

---

In Partial Fulfillment
of the Requirements for the Degree
Masters of Science
Bioengineering

---

by
Neil Travis
May 2007

---

Accepted by:
Ted Bateman, Ph.D., Committee Chair
Jiro Nagatomi, Ph.D.
Lisa Benson, Ph.D.

## ABSTRACT

Radiation exposure is experienced in both radiotherapy and exploratory space missions. As cancer treatments improve and astronauts aim to explore beyond low earth, radiation's effects on bone must be clearly understood. Nine-week old female C57BL/6 mice were evaluated for cortical bone changes by mechanical testing, micro-computed tomography, quantitative histomorphometry, percent mineralization and micro-hardness indentation. Study one, Multi-Type study, mice received a 2 Gray (Gy) gamma, proton, iron and carbon whole body radiation dose and sacrificed 110 days post-exposure. Study two, High-Dose study, mice received a 7 Gy gamma radiation whole body dose and sacrificed 14 days post-exposure. Neither study revealed significant difference between irradiated nor control groups for any assay. Sublet effect between high Linear Energy Transfer (LET) and low LET radiation was observed. Lack of changes to cortical bone is particularly interesting and may indicate a unique biological microdosimetry microenvironment. This thesis specifically examines radiation effects on cortical bone.

## DEDICATION

This thesis is dedicated to all those who have made this possible for me. My parents for providing support throughout school to achieve and teaching me the value of hard work through out those so many years. Also, for putting up with what it takes to have me achieve something difficult.

I would also like to dedicate this to the teachers and family that have helped to shape me into who I am today.

## ACKNOWLEDGMENTS

There are many people who must be acknowledged in accordance with this work. I would like to acknowledge Dr. Ted Bateman for running the Osteoporosis Biomechanics Laboratory, and providing me the direction and support to complete this work. Also, fellow graduate students Jeffery Willey, Eric Bandstra for assisting me in the figuring out and learning many fundamentals to my research, Felicia Bateman, Laura Smith, Dr. Paul Coe and Edward De Iulio for editorial support. Lisa De Iulio as well, for supporting and helping where possible. Also, acknowledge my committee members Dr. Lisa Benson and Dr. Jiro Nagatomi. Funding from National Space Biomedical Research Institute, Proctor and Gamble and the South Carolina Space Grant Consortium for making this work possible.

**TABLE OF CONTENTS**

Table of Contents (Continued)

Table of Contents (Continued)

Page

## LIST OF TABLES

## LIST OF FIGURES

List of Figures (Continued)

Page

# CHAPTER 1

# INTRODUCTION

## 1.1 General Bone Biology

### 1.1.1 Material Composition

Bone is a dynamic body system with multiple functions composed of several distinct parts. Bone supports and protects soft tissues, assists with movement, stores minerals, and provides a primary site for blood cell formation. (Marieb, 2004). It is composed of 70% mineral (hydroxyapatite), 22% proteins (type I collagen), and 8% water by weight (Augat and Schorlemmer, 2006). Strength is determined by the quality of these components and their spatial makeup within bone. Collagen, specifically type I, is an important component in the material makeup of bone. Orientation and quality give bone the ability to withstand tensile loading (Viguet-Carrin et al., 2006). The degree to which bone is mineralized helps determine the structural stiffness possible within the material. Bone mineralization is made up of various sizes crystals. These crystals surround and attach to the collagen fibers using noncollagenous proteins giving bone compressive strength and hardness. As bone ages these crystals typically become larger and the bone becomes more brittle. These mineral and collagen components comprise the materials that are involved within bone and determine its strength characteristics.

### 1.1.2 Structural Composition

There are two primary types of bone: cortical and trabecular (cancellous). Comprising about 80% of the skeleton (by mass), cortical bone is located in the shafts and outer surface of long bones and flat bones. Its unique geometry provides a strong

material for both structural support and loading within the body. It undergoes advanced mineralization and a slower turnover rate than trabecular bone. The outer surface of cortical bone, the periosteal surface, contains precursor bone cells and nutrients.

The middle of long bones, such as the femur, contains hollow areas which are filled with marrow. Surrounding the marrow cavity is cortical bone. This marrow is home to many of the stem cells of the immune system. The bone's inner surface, where bone and marrow interact, is referred to as the endosteal surface. Cortical bone is vascularized through haversian canals in larger mammals such as humans. Haversian canals are series of tubes formed within osteons where blood vessels and nerve cells reside. The cortical bone of mice and rats is not vascularized in the same way and receives its nutrients from the surrounding vessels and the marrow.

This haversian system in larger mammals also creates increased intracortical porosity which contributes 70% of the elastic modulus and 55% of the yield stress (Dong and Guo, 2004). Elastic modulus represents the ability to deflect and withstand a certain load and be able to return to the original geometry after the load is removed without fracturing, up to a maximal load. Yield stress is determined as the stress at which the material exits the elastic region and plastic deformation of the material occurs fracturing of the bone occurs. The ability to withstand fracture decreases significantly with an increase in porosity (Augat and Schorlemmer, 2006). Cortical bone is considered the primary structural support in bone and knowledge of this bone type is important in the evaluation of overall bone strength.

The other type of bone is trabecular. This bone is located in the epiphyses of long bones, the middle section of flat bones, and in the middle of vertebrae. This type of bone

is molecularly the same as cortical bone; however, it does not contain haversian canals for vascularization. It redistributes applied loads and adds stability to bone. Trabecular bone is anisotropic and contained within the endocortical section of cortical bone. It is typically less mineralized and has a much higher turnover rate than cortical bone (Heaney 2003). Studies have shown trabecular bone to provide an 11- 57% mechanical contribution to the vertebrae of rats (Ito et al., 2002), with a 50- 70% contribution to loading strength in human vertebrae (Homminga et al., 2001). Both cortical and trabecular bone provide a unique and significant contribution to the overall well being of bone which necessitates a specific evaluation of each type.

### 1.1.3 Bone Remodeling

Bone's continuously remodeling characteristic makes it dynamic. The remodeling process is the breakdown/resorption of existing bone and the laying down/formation of new bone in the place of the old (Hadjidakis and Androulakis, 2006). There are three main cell types within bone: osteoclasts, osteoblasts and osteocytes. Osteoclasts and osteoblasts accomplish bone restoration in a coordinated manner referred to as coupling. In the remodeling process, osteoclasts resorb bone after which the osteoblasts lay down a matrix of collagen and organic material. Initially the material deposited by the osteoblast is called osteoid. It mineralizes and matures into bone. Osteocytes are cells located within the bone matrix rather than on its surfaces. These cells are less spatially dense per area within the boney tissue compared to cells in the surrounding soft tissue and marrow.

In theory, these remodeling activities are mediated by the bone’s loading situation and the age necessitating resorption. As previously discussed, the osteoclast is responsible for bone resorption and the osteoblast is responsible for formation of new

osteoid (Hadjidakis and Androulakis, 2006). Over time this osteoid matures into mineralized bone. Osteocytes were formerly osteoblasts that were incorporated within the bone matrix as formation occurs. This cycle of bone remodeling is shown in Figure 1.1. These osteocytes are believed to assist in signaling resorption of bone in specific areas through apoptosis, programmed cell death (Noble, 2003). This prevents accumulation of micro-cracks in enough quantity to cause material failure. These micro-cracks are remodeled within bone and studies are currently underway to determine the mechanism by which osteoclasts are stimulated to initiate resorption of specific portions of bone (Gu et al., 2005; Noble, 2005). It is estimated between 2% and 5% of bone is remodeled each year (Hadjidakis and Androulakis, 2006). Remodeling is a necessary process to keep bone structurally sound and able to withstand daily life stresses.

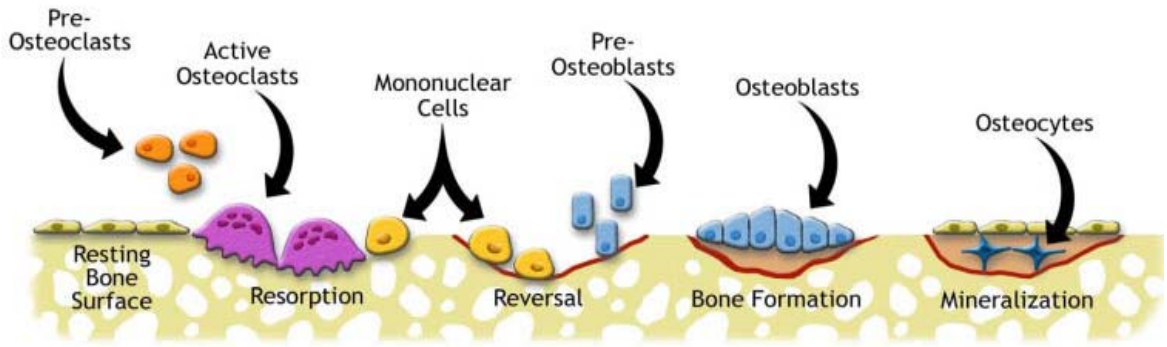


**Figure 1.1:** The remodeling cycle of bone, (http://www.umich.edu/news/Releases/2005/Figure 1Feb05/bone.html)

### 1.1.4 Biomechanics

Collectively, bone's structural and material components provide the body's functional support. Collagen fibers with a longitudinal orientation contribute to a bone's bending strength to increase resistance to tension (Robling et al., 2006). Additionally, these collagen fibers are crosslinked at specific angles ($45^{o}$ and $135^{o}$) to further strengthen

bone in tensile loading. Crystals, formed during mineralization, help provide stiffness and resist compression.

Structurally, several characteristics improve a bone's strength. The vertical arrangement of haversian canals and osteons improves strength in the load bearing ability of the bone in response to body weight (Marieb, 2004). An osteon is the compact bone structural unit. They are elongated cylinders functioning as "pillars" within bone (Marieb, 2004). Osteons are built by concentric tubes like a tree trunk, one outside the next and each tube is a lamella (Marieb, 2004). The collagen fibers are angled a single way ($45^{o}$ or $135^{o}$) in each lamella. Surrounding each osteon are cement lines marking the end of the osteon. The cement lines, along with the osteon, help limit crack propagation within the boney material to prevent fracture.

The bone as a whole is optimized for maximum efficiency, with the thicker material on the outer surfaces and the hollow inner marrow cavity. Using area moment of inertia calculations, material on the inner section of a rod-like shape is a smaller contributor to strength than the material distributed in a tube shape (Figure 1.2). Long bones are especially similar to this geometrical arrangement. A rod and tube with the same area are as shown in Figure 1.2. The hollow tube is stronger because more material is distributed to the area requiring maximum load resistance and not wasted in the center where the least amount of load is transferred, in bending or torsion. Cortical bone is arranged in this manner to provide maxim strength where it is needed and minimal resistance where load is lightest. As porosity increases in cortical bone, strength decreases.

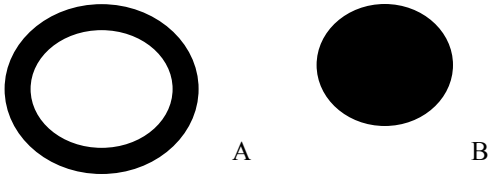


| | Area | Area Moment of Inertial |
|---|---|---|
| (A) | 12.6 $cm^2$ | 378.1 $cm^4$ |
| (B) | 12.6 $cm^2$ | 125.7 $cm^4$ |

**Figure 1.2:** Representation of a tube and a rod, which respective moment of inertias. (A) Representation of tub (bone), (B) Representation of a regular rod. The areas of these figures are represented by the black and are assumed to be equal. These two figures show the difference in arrangement of bone within the long bones. It has the material moved to the outer areas that carry more load and no material is being wasted in the center.

The trabecular bone within the marrow cavity of long bones and vertebrae is arranged to resist maximum stresses of daily loading. It is arranged anisotropically to withstand loading in specific directions, which are applied by normal forces produced by the body. Structurally, the trabeculae are rods or plates, making them able to withstand bending better in one direction than another. These specific characteristics of bone provide for a structurally sound material.

### 1.1.5 Osteoporosis

Osteoporosis is characterized by low bone mass and micro-architectural deterioration leading to bone fragility and increased fracture risk (Lamichhane, 2005). In type I osteoporosis trabecular bone loss is accelerated, while in type II osteoporosis both cortical and trabecular bone are lost in equal proportions (Lamichhane, 2005). Type I occurs in postmenopausal women initiated by a reduction in estrogen producted. Type II or senile osteoporosis occurs in older individuals regardless of sex. Spaceflight osteoporosis occurs when astronauts in micro-gravity do not maintain normal loads on

their limbs from the reduced gravity. In addition, spaceflight is unique since osteoblasts and osteoclasts are uncoupled during resorption resulting in an overall rapid loss of bone (Smith et al., 2005). This exceptionality could provide opportunities to study the mechanisms causing osteoporosis over a relatively short time period. Evaluations and preventive measures developed to diagnose and arrest or prevent spaceflight induced osteoporosis could lead to improved diagnosis, therapy, and prevention for people at risk in the general population.

A majority of diagnosed cancer is found in those 65 years old or older (Baxter et al., 2005; Pollack et al., 2005). Therapeutic use of radiation for cancer therapy in people over 65 may increase the risk of developing osteoporosis in a segment of the population already at a higher risk due to age associated bone loss. More than 1% of people 50 years or older will fracture a hip (Kanis et al., 2003) and caucasian women 50 years or older have a 17% chance of developing a hip fracture from osteoporosis (Melton, 2000). Patients who fracture a hip are at increased risk of fatality (Kanis et al., 2003). A significant health obstacle exists when older patients who are already at greater risk for fracture are exposed to radiation's damaging effects.

## 1.2 Radiation

Humans are exposed to radiation beneath clinical levels in their everyday life. This background radiation, around 0.5 milli-Gray per year (mGy/year), is not sufficient to cause measurable health problems (Todd, 2003). A Gray (Gy) is the International System of Units (SI) unit of absorbed dose and is measured in Joules/kilogram. Exposure

to physiological harmful doses of radiation can occur in a number of ways. Two important radiation exposures are from cancer patients undergoing therapeutic medical irradiation and exposure to astronauts while exploring outer space.

### 1.2.1 Radiotherapy in Cancer Patients

Diagnoses of an estimated 1.4 million new cases of cancer are expected in 2006 (American Cancer Society, 2006). The estimated five year survival rates for all stages of breast, colon, and prostate cancer are 88.2%, 64.1%, and 99.8% respectively (American Cancer Society, 2006). Approximately 50% of cancer patients are treated with radiation during therapy for the disease (Bentzen, 2006; Radiological Society of North America, 2005). Prior studies indicate increased risk of bone fracture associated with radiation exposure (Baxter et al., 2005; Hamilton et al., 2006a; Maeda et al., 1988; Mitchell and Logan, 1998; Nyaruba et al., 1998; Sugimoto et al., 1991). Cancer patients typically receive small doses of radiation, approximately 1-2 Gy per dose, in repeated treatments over time to build up sufficient radiation in the body to kill cancer cells (40-70 Gy local to tumor) (Bolek et al., 1996; Rohrer et al., 1979). A typical regimen would include daily treatments five days per week for two to nine weeks. Depending on the patient and type of cancer, therapy might be performed twice a day. Bone marrow is devastated by radiation, drastically reducing the supply of stem cells needed to support the immune system (Robling et al., 2006; Sugimoto et al., 1991). This can be an undesirable consequence or, in the case of a bone marrow transplant, an intentional effect to eliminate function (Banfi et al., 2001).

A problem currently under clinical investigation is the bone weakening and small fractures in the pelvic region observed following radiation therapy for certain cancers,

such as prostate or colon cancer (Baxter et al., 2005; Rex and Elsworth, 1998). Gamma/X-ray, or less commonly, proton radiation is typically used in medical procedures. As treatments improve and patients live longer, understanding and anticipating post-treatment bone damage becomes increasingly important to prevent serious complications.

### 1.2.2 Spaceflight Application

During long-duration (4-6 months) stays aboard the International Space Station astronauts experience a rapid rate of bone loss within the femora and vertebrae (0.9 - 1.6% per month) (Lang et al., 2004). Specific locations within the skeleton, such as the calcaneous, could experience losses exceeding 2% per month (Tilton et al., 1980). Bone loss during unloading is caused by an increase in resorption compounded by reduced calcium consumption, reduced intestinal calcium absorption, and increased calcium excretion (Smith et al., 2005). During spaceflight, an uncoupling of bone resorption and formation occurs. Analyses of alkaline phosphatase and osteocalcin levels indicate that bone formation remains steady or declines slightly instead of moving in parallel with resorption (Smith et al., 2005). Exercise can prevent bone loss in micro-gravity to a limited degree (Goodship et al., 1998).

In additional, there is incomplete load bearing skeletal recovery up to a year after returning to Earth (Lang et al., 2006; Vico et al., 2000). Bone volume and cross-sectional area increases to support the greater loads from the return to gravity and to compensate for the loss of trabeculae and bone density, but strength is not completely returned to pre-flight values (Lang et al., 2006). This increase in volume is an accelerated form of bone adaptation also seen in aging (El-Kaissi et al., 2005). Astronauts lose a significant

portion of bone while in micro-gravity and require further evaluation to understand and treat this phenomenon.

#### 1.2.2.1 Radiation and Spaceflight

In addition to skeletal changes due to microgravity, astronauts on exploratory missions to the Moon and Mars will be exposed to elevated levels of radiation. Once astronauts leave low earth orbit on exploratory missions, they will be exposed to high charge and energy (HZE) particles and proton radiation from solar particle events (SPE), solar flares and cosmic events (Benton and Benton, 2001; Blakely, 2000). Space radiation is complex, with components ranging from protons to iron particles, accompanied by secondary radiation, such as, Bremmstrahlung x-rays and neutrons (Epelman and Hamilton, 2006; Heilbron et al., 2005). One major source of radiation is cosmic rays consisting of heavy ions and protons (Benton and Benton, 2001; Blakely, 2000; Townsend, 2005). Another, major source of space radiation is solar particle events (SPE) consisting primarily of protons. Solar sources are often unpredictable and can result in a higher exposed doses over a shorter time (Benton and Benton, 2001; Blakely, 2000; Stephens et al., 2005).

Unprotected, astronauts could be exposed to potentially lethal doses of radiation. A total body dose of approximately 2.5 Gy can be lethal to humans with out significant medical intervention (Todd, 2003). Depending on shielding, duration of mission, and solar activity a dose of approximately 1 – 2 Gy can be expected on a mission to Mars or 0.1 – 2 Gy for a shorter mission to the Moon (Foullon, 2004; Moore, 1992; Parsons and Townsend, 2000; Simonsen et al., 1993; Stephens et al., 2005). Radiation's effects on

bone already compromised by micro-gravity are not well described in the current scientific literature.

#### 1.2.2.2 Radiation Types of Spaceflight

Ionizing radiation originates from many sources. Radiation encountered during spaceflight is qualified as low and high linear energy transfer (LET). This physical parameter measures the mean rate of energy deposited locally along the track of a charged particle by electromagnetic interaction (Blakely, 1984). Low-LET as found in medical and space applications consists of lighter particles with a lesser charge and a less linear ionizing track. High-LET is typically encountered only beyond low earth orbit space travel and consists of heavy higher charged particles that create exceptionally linear ionizing tracks. High-LET radiation is of particular concern because of the particles size involved. The energy deposited by the nucleus of an iron (high-LET) particle leaves a trail through tissue on the order of tens of micrometers wide while a typical mammalian cell nuclei is only several micrometers in diameter (Simonsen et al., 2000). A single iron nucleus could have potentially injurious effects when it passes through tissue. High-LET appears to have a higher potential for tissue damage, while the more extensively tested low-LET has shown to have a negative effect on bone strength.

## 1.5 Cortical Bone Examination

Despite the increased fracture risk experienced by cancer patients receiving radiation therapy, little research is available to define the causal mechanisms at the cellular, molecular or structural levels. Few studies describe changes in cortical bone at lower/moderate radiation doses (0.5 – 7 Gy). One study describes reduced cortical bone strength following high doses (30 – 50 Gy) of site specific radiation (Nyaruba et al.,

1998). Fractionated doses do not seem to have as much an effect on cortical bone strength as a single large dose (Nyaruba et al., 1998; Rohrer et al., 1979). The fractionated dose is similar to clinical radiation in its administration and could provide insight into cortical bone behavior following such exposures. Radiation encountered in space is at a low dose but is accumulative in nature since longer missions will result in more exposure. Furthermore, there is a possibility of high dose exposure from solar flares, solar particle events and structural failure of equipment and/or craft.

## 1.7 Previous Examinations of Trabecular Bone

Recently, a profound loss of trabecular bone after 2 Gy exposure to gamma, proton, carbon and iron radiation types was reported. Trabecular volume fraction was significantly reduced following exposure to gamma (29%), proton (35%), carbon (39%), and iron (34%) radiation when compared to the control group (Figure 1.3) (Hamilton et al., 2006b). Trabecular connectivity declined after exposure to proton (64%), gamma (54%), carbon (54%), and iron (46%) versus the control (Hamilton et al., 2006b). Moreover, trabecular thickness increase after gamma (5%), proton (6%) and decreased significantly in response to carbon (10%) and iron (11%) radiation (Hamilton et al., 2006b). With a sacrifice point of four months after exposure, the data suggests considerable damage to the trabecular bone, since this is well outside the range of an acute physiological reaction.

In a further study, a rapid decline in trabecular bone, two weeks following high dose irradiation of 7 Gy was seen (Figure 1.4) (Willey et al., Submitted 2007). Trabecular volume fraction decreased by 54% and trabecular connectivity density decreased by 69% but there was no difference in the trabecular thickness. Histology

indicated osteoclast and osteoblast surfaces were not different suggesting a very rapid response after high dose radiation.

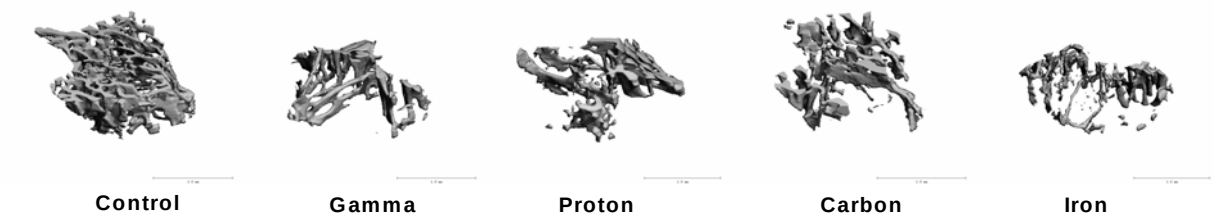


**Figure 1.3:** MicroCT images of the proximal tibia after multiple types of radiation at 2 Gy doses of radiation (Hamilton et al., 2006b)

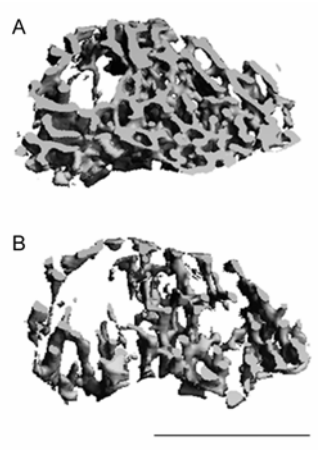


**Figure 1.4:** MicroCT images of trabecular bone in the proximal tibia after 7Gy of Gamma radiation, (A) control and (B) 7 Gy (Willey et al., Submitted 2007)

The data in the two studies presented are clinically applicable for cancer patients receiving radiation treatment as well as astronauts exposed to radiation during space exploration. Cancer patients are living longer after radiation treatment with 88.5% (breast), 64.1 % (rectal and colon) and 99.9% (prostate) five year survival rates (American Cancer Society, 2007; MMWRMorbMortalWklyRep, 2004). Many of these patients will receive radiation during the course of treatment for the disease (Bentzen, 2006). Astronauts are exposed to space radiation such as solar particle events during

periods of high solar activity as well as microgravity, both of which contribute to bone loss. Both radiation exposures are potentially hazardous to health and wellbeing. Radiation exposure resulted in a profound loss of trabecular bone; however, preliminary cortical parameters evaluations revealed no differences. A thorough examination of cortical bone properties is needed. The objective of the research conducted for this thesis was to determine the affects of different radiation types and doses on cortical bone.

# CHAPTER 2

## RESEARCH GOALS

Previous studies demonstrated striking trabecular bone loss following radiation exposure at 2 and 7 Gy (Hamilton et al., 2006b; Willey et al., Submitted 2007). Trabecular volume fraction was reduced 29-39% after exposure to a 2 Gy dose of multiple types of radiation and 54% of trabecular volume fraction was lost after a high 7 Gy dose of gamma radiation (Figure 1.3 and 1.4). These studies represent both a long term study with a lower/moderate dose of multiple types of radiation and a short term study with a single high dose of radiation. The demonstrable losses in trabecular bone exemplify the need for specific evaluation of the effects on each bone type. This study augments previous research by incorporating more detailed analysis of changes observed following irradiation of different radiation types.

A complete understanding of the biological reaction to irradiation has not yet been established using the results for these two studies. The prior studies emphasized the effects on trabecular bone. Thus, cortical parameters need further examination after significant losses of trabecular bone as cortical bone plays an important role in overall bone strength. The goals of this thesis are to more fully describe the effects of radiation on the mechanical, material and structural properties of diaphyseal cortical bone.

Goal One: Examine the properties of diaphyseal cortical bone to determine long-term changes associated with exposure to a 2 Gy dose of multiple radiation types applied in single doses to the whole body.

The first study termed the “Multi-Type study” exposed mice to both radiotherapy

and space-relevant methods of radiation exposure, and the examination of diaphyseal cortical bone will be performed with several analyses representing mechanical, structural and material properties. Four radiation types were used: gamma, proton, iron and carbon, all applied as a 2 Gy whole body dose. Mice were sacrificed approximately 4 months (110 days) after exposure. This longer period of time after exposure allowed evaluation of chronic, and potentially permanent, skeletal changes following irradiation. The different types of radiation were applied as high-LET (carbon and iron) and low-LET (gamma and proton). Previously, these different radiation energies demonstrated an LET effect with trabecular thickness (Hamilton et al., 2006b): determining a potential LET effect on cortical bone is an important sub-aim of the Multi-Type study.

Goal Two: Examine the properties of diaphyseal cortical bone to determine short-term changes associated with exposure a single 7 Gy dose of gamma radiation.

The second study termed the "High-Dose study" was designed to expose mice to higher doses of radiation comparable to those encountered in therapeutic procedures, and the examination of diaphyseal cortical bone will be performed with the same techniques representing mechanical, structural and material properties. A whole body dose of gamma radiation was applied at a 7 Gy dose. This study evaluated the short-term effects of radiation with animals being sacrificed 2 weeks (14 days) post-irradiation. This dose was a high single dose of radiation and represents an extreme case of radiation exposure.

# CHAPTER 3

# DIFFERING EFFECTS OF HIGH AND LOW-LET ON DIAPHYSEAL CORTICAL BONE

N.D. Travis[1], M.J. Pecaut[2], D.S. Gridley[2], Jeffrey Willey[1], Eric Bandstra[1], Greg Nelson[2] and T.A. Bateman[1]

[1]Bioengineering Department, Clemson University, Clemson, SC

[2]Loma Linda University and Medical Center, Loma Linda, CA

**Data related to this chapter will be submitted in manuscript form to Aviation, Space and Environmental Medicine.**

We have recently identified a profound and prolonged loss of trabecular bone (29-39%) in mice exposed to 2 Gray (Gy) doses of multiple radiation types, representing modeled exposure from both solar and cosmic sources. The microgravity component of spaceflight environment coupled with radiation exposure may place astronauts at a greater risk for mission critical fractures. To evaluate bone strength each component, cortical and trabecular bone, must be considered. Skeletal strength is a complex composite consisting of both trabecular and cortical bone. The aim of this paper is to examine mechanical, structural, and material properties of cortical bone exposed to multiple types of radiation. The study was conducted on nine-week old female C57BL/6 mice exposed to a 2 Gy whole body dose of gamma, proton, iron and carbon radiation and sacrificed 110 days post exposure. Femora were evaluated by mechanical testing, micro-computed tomography, quantitative histomorphometry, percent mineral content, and micro-hardness. A high-LET effect was observed; carbon and iron (high-LET)

radiation types caused declines in structural properties compared to low-LET radiation (gamma and proton). However, despite the previously reported profound loss of trabecular bone caused by these radiation types, when compared to non-irradiated control mice, no statistically significant differences were observed in mechanical, structural, and material properties for any radiation type. The LET effects require further investigation to identify time course and initiating mechanisms. A much greater effect of radiation on trabecular bone is of particular interest and may indicate a unique biological microenvironment of microdosimetry conditions that is not only specific to bone, but to trabecular bone.

## 3.1 Introduction

Trabecular bone loss was recently reported after 2 Gray (Gy) irradiation (Hamilton et al., 2006b). In this study, trabecular volume fraction was significantly reduced following exposure to gamma (29%), proton (35%), carbon (39%), and iron (34%) compared to the control group (Hamilton et al., 2006b). Trabecular connectivity declined after exposure to proton (64%), gamma (54%), carbon (54%), and iron (46%) versus controls (Hamilton et al., 2006b). Additionally, trabecular thickness changed increasing after gamma (5%) and proton (6%) and decreasing significantly in response to carbon (10%) and iron (11%) irradiated groups (Hamilton et al., 2006b). In a further study, trabecular volume fraction declined (54%), in just two weeks following high dose irradiation (7 Gy) (Willey et al., Submitted 2007). Although profound losses of trabecular bone were observed the preliminary evaluation of cortical bone parameters revealed no differences. A thorough examination of cortical bone properties requires additional in-depth analysis.

### 3.1.1 Spaceflight

Astronauts on long-duration (4-6 months) stays aboard the International Space Station experience a rapid rate of bone loss within the femora and vertebrae (0.9 - 1.6% per month) (Lang et al., 2004). Specific bone locations, the calcaneous, could experience losses exceeding 2% per month (Tilton et al., 1980). This loss during unloading is caused by an increase in resorption compounded by the effects of reduced calcium consumption, reduced intestinal calcium absorption, and increased calcium excretion (Smith et al., 2005). During spaceflight, an uncoupling of bone resorption and formation occurs. Analysis of alkaline phosphatase and osteocalcin established bone formation actually

remains steady or declines slightly instead of moving in parallel with resorption (Smith et al., 2005). Exercise can only prevent bone loss in microgravity to a limited degree (Goodship et al., 1998). Also, there is incomplete load bearing skeletal recovery up to a year after returning to Earth (Lang et al., 2006; Vico et al., 2000).

### 3.1.2 Radiation and Spaceflight

During exploratory missions to the Moon and Mars astronauts will be exposed to both microgravity and radiation. The nature of space radiation is complex, with components ranging from protons to iron particles, accompanied by secondary radiation (e.g. Bremmstrahlung x-rays and neutrons) (Epelman and Hamilton, 2006; Heilbron et al., 2005). One predominate source of radiation is cosmic rays which consists of heavy ions and protons (Benton and Benton, 2001; Blakely, 2000; Townsend, 2005). Another, predominate source of space radiation is solar particle events (SPE) consisting primarily of protons. Solar sources are more unexpected and can result in a higher exposed dose in a shorter time (Benton and Benton, 2001; Blakely, 2000; Stephens et al., 2005). Unprotected, astronauts could experience potentially lethal doses. A dose of approximately 1 – 2 Gy can be expected on a mission to Mars or a dose of 0.1 – 2 Gy for a shorter mission to the Moon within a spacecraft depending on: shielding, mission duration and/or solar activity (Foullon, 2004; Moore, 1992; Parsons and Townsend, 2000; Simonsen et al., 1993; Stephens et al., 2005). Radiation's effects on bone already compromised by microgravity are not clear.

### 3.1.3 Contribution of cortical and trabecular bone

The contributions of cortical and trabecular bone to overall skeletal strength are complex, and not completely understood. While cortical bone is considerably denser than trabecular bone and is viewed as a greater determinant of strength, both bone types play fundamentally important roles. Trabecular bone contributes 11% - 57% of the mechanical strength in the vertebrae of rats (Ito et al., 2002) and 50% - 70% to the strength in human vertebra (Homminga et al., 2001). Cortical and trabecular bone each play important roles in the strength of bone. Specific evaluations of both bone components are necessary to evaluate the overall affects of radiation on bone strength.

### 3.1.4 Radiation and Cortical Bone Changes

Previously published studies describe deleterious effects to cortical bone following radiation. A high, single dose of 30 - 50 Gy, significantly reduced cortical bone strength (Maeda et al., 1988; Nyaruba et al., 1998; Sugimoto et al., 1991). However, fractionated smaller doses do not produce the same reductions in strength (Nyaruba et al., 1998; Rohrer et al., 1979). The purpose of this paper is to examine the effects on cortical bone at lower/moderate dose radiation such as might be encountered during spaceflight exposure.

## 3.2 Methods

### 3.2.1 Animals

This study was conducted using nine-week old female C57BL/6 mice (Charles River Breeding Labs, Wilmington, MA). Animals were acclimatized for one week prior to irradiation, with food and water available ad libitum. The Institutional Animal Care and use Committees of both Loma Linda University Medical Center and Brookhaven National Laboratory approved all study procedures.

The hind limbs were removed from the animals post euthanasia. Samples were transported from Loma Linda, California at -20$^{o}$ C. The femur and tibia were then separated and each cleaned of non-osseous tissue.

### 3.2.2 Irradiation

Prior to radiation, the animals were placed into individual rectangular polystyrene boxes with air holes (30 mm x 30 mm x 85 mm) (Gridley et al., 2002). Four groups of mice each received whole-body irradiation from one of four types of radiation. Group 1 (n=10) was exposed to 60-Cobalt ($^{60}$Co) gamma rays, linear energy transfer (Vico et al.) = 0.23 keV/micron. Group 2 (n=10) was exposed to protons ($^{1}H^{1+}$, 250 MeV/n), LET = 0.4 keV/micron. Group 3 (n=9) was exposed to carbon ($^{12}C^{6+}$, 290 MeV/n), LET = 13 keV/micron. Group 4 (n=9) was exposed to iron ($^{56}Fe^{26+}$, 1 GeV/n), LET = 148 keV/micron. A control group (n=10) was not irradiated.

Low-LET exposures ($^{60}$Co and protons) were performed at Loma Linda University Medical Center as previously described (Gridley et al., 2002; Hamilton et al., 2006a).

For $^{60}Co$ irradiation, a horizontal beam from a retired AECL (Atomic Energy of Canada, Ltd.; Commercial Products Division; Ottawa, Canada) Eldorado therapy unit was used. Protons were delivered in 0.3 s pulses every 2.2 s. High-LET exposures (C and Fe) were performed at the Brookhaven National Laboratory in the NASA Space Radiation Laboratory according to standardized procedures. All irradiations were delivered as 25-40 pulses per minute to yield a cumulative 2 Gy with average dose rates ranging from 0.6 to 1.2 Gy/min. Particle radiation (proton, carbon, and iron) was delivered at the entrance plateau region of the beam, at the beginning of the Bragg Peak, such that LET levels were held constant throughout the target volume.

Four to eight unanesthetized mice were irradiated simultaneously. The irradiation conditions were coordinated between investigators at the two facilities. Thus, exposures were performed with uniform procedures and fixtures. Euthanasia and tissue harvesting occurred at a similar times post exposure. The mice irradiated at Brookhaven National Laboratory were shipped within days to Loma Linda University for housing and analysis. Animals were euthanized with 100% $CO_2$ at 110 days post exposure as previously described (Hamilton et al., 2006b; Pecaut et al., 2000).

### 3.2.3 Analysis

3.2.3.1 Mechanical Testing**:** Harvested femora were soaked in sodium chloride for 1.5 hours prior to testing (Broz et al., 1993). A three-point bending test examined mechanical properties of the femora at the mid-diaphysis using an Instron 5582 (Instron Corporation, Norwood, MA), with a 50 N load cell (0.05 N resolution) and Bluehill 2 (Instron Corporation, Norwood, MA) software. Femora were loaded to failure using an anvil with a 9 mm span length. The femur was placed with condyles facing upward in

the anvil with a deflection rate of 5 mm/min. Force (Newtons, N) and deflection (millimeter, mm) (Homminga et al.) were collected at 10 Hz. Custom written software was used to determine the elastic limit ($P_e$), maximum force ($P_m$) and force at fracture ($P_f$) from the measured values. Stiffness (S) analyzed from obtained force deflection curves. Figure 3.1 represents an idealized load deflection curve with the points marked.

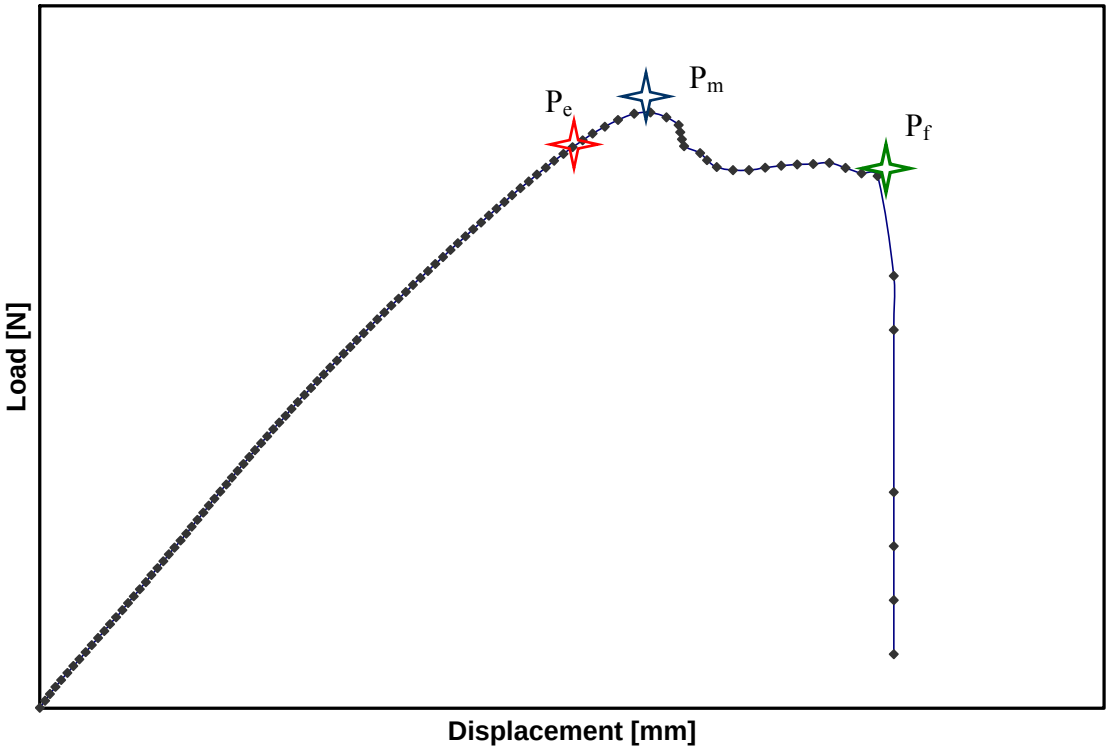


**Figure 3.1:** This figure represents an idealized load versus displacement curve for the output of the mechanical data measure. The points mark the places on the curve where mechanical values were determined.

3.2.3.2 Micro-computed Tomography Properties: Femora were removed and cleaned of non-osseous tissue in preparation for micro-computed tomography (microCT) analysis (*microCT20*, Scanco Medical AG, Bassersdorf, Switzerland). Bones were analyzed to determine maximum, minimum and polar moments of inertia, cortical porosity and cortical volume. One hundred and five slices of the diaphysis were scanned (the span of

the diaphysis that was mechanically tested), each slice having a thickness of 9 microns with 100 microns between each slice. Scans were initiated at the base of the femoral neck and sequentially to isolate the junction of the femoral neck and diaphysis for a starting reference point. A total of 91 slices (approximately 9mm) were evaluated distal to this established reference point. Multiple parameters were examined evaluate structural maintenance of cortical bone.

3.2.3.3 Quantitative Histomorphometry: After being cleaned of non-osseous tissue, the femora were placed in neutral buffered 10% formalin for 48 hours then immersed in 70% ethanol, for preservation until needed for assay. Prior to testing the bones were dried for two days. Femora were measured from the proximal end of the ball on the femoral head to the distal end of the femoral condyles. Bones were embedded in Non-infiltrating Epo-Kwick epoxy (Buehler Ltd., Lake Bluff, IL) and allowed to dry for 24 hours prior to cutting. Femora were cut distally to the third trochanter (Buehler, 12.7 cm x 0.5 cm diamond blade). Disk sections were polished using 600, 800, 1200 grit carbide paper and diamond paste. The femora sections were viewed on a Zeiss Axioskop 2 plus (Carl Zeiss MicroImaging, Inc., Thornwood, NY) with AxioVision software for digital imaging. SigmaScan Pro 5 (Systat Software, Inc., Point Richmond, CA) software was used to analyze the specimens. Individual bones were viewed at 5X magnification under UV light with a Fs 05 filter. The major and minor axis diameters were identified and measured. The perimeters of the endocoritcal (Ec.Pm) and periosteal (Ps.Pm) surfaces were traced and analyzed for area (Ec.Ar, Ps.Ar) and lengths. Cortical area was

calculated by subtracting the endocortical area from the periosteal area (Ct.Ar = Ps.Ar. – Ec.Ar).

3.2.3.4 Compositional Analysis: Femora in this study were examined to analyze the percent mineral composition. The bones were reduced to ash using an Isotemp Muffle furnace (Fisher Scientific Company L.L.C., Pittsburgh, PA) in order to assess mineral composition within each bone. Proximal and distal epiphyses were separated from the diaphysis and weights were recorded. Each component was then positioned in the oven at 105$^{o}$C for 24 hours, after which weights were again recorded (dry mass, Dry-M). Bones were then baked at 800$^{o}$C for 24 hours, and reweighed (mineral mass, Min-M). Organic mass (Org-M) was calculated by subtracting mineral mass from dry mass (Org-M = Dry-M – Min-M). The percent mineral content was calculated as Min-M/Dry-M*100%.

3.2.3.5 Micro-Hardness Indention: Micro-hardness indentation was assessed using the femora from the same bones and disks utilized during the quantitative histomorphometry. Bones were analyzed using a Buehler Micromet 5101 micro-hardness indenter (Buehler, Lake Bluff, IL). The indentions were performed on the lateral side of each bone. Four indentions were made with a 40 μm spacing from the periosteal surface and between each indention. The length and width of each indention was measured and recorded, addition information can be found in Chapter 4, Section 4.2.2.5. An average value was then calculated from micro-hardness measurements made on each bone. Vicker's method was used to calculate the hardness of each bone (Callister, 2007) and compared to the control

group. Vicker's hardness is calculated with respect to the magnification of the ocular at the time of measurement and by the average of the length and width of the diamond shaped indention.

3.2.3.6 Statistics: Statistical analysis were performed using SigmaStat software version 3.5 (Systat Software Inc., Richmond, California), using a one-way ANOVA with a Tukey's follow up test. Alpha was set at 0.05, $\alpha = 0.05$. To signify a trend $0.05<P<0.01$ was used. The primary goal of statistics was to compare the irradiated groups to the control groups. Subsequently, the Tukey's follow-up test compares all groups to one another and differences between each group can be observed.

## 3.3 Results

Animal mass and femoral lengths were not different between any irradiated groups and control group. No differences in mechanical strength were observed compared to the controls (Table 3.2). Additionally, no differences were identified between moments of inertia, cortical volume or cortical porosity compared to the controls (Figure 3.2). Endocortical area (Figure 3.3) and cortical area in irradiated groups were not statistically different from control groups (Table 3.2). However, a trend towards increased endocortical area was observed between carbon and control groups (Figure 3.3). Compositional analysis (Figure 3.4) and micro-hardness were shown to have no difference between irradiated groups and the control. Cortical morphometric parameters are listed in Table 3.1.

**Table 3.1:** Mechanical testing data from Multi-Type study**.**

| | | | Force (N) | | | | | |
|---|---|---|---|---|---|---|---|---|
| **Treatment** | **Stiffness (N/mm)** | | **Elastic** | | **Maximum** | | **Fracture** | |
| Control | 30.84 | ±2.82 | 13.32 | ±0.917 | 16.82 | ±0.404 | 12.15 | ±0.844 |
| Gamma | 34.55 | ±2.64 | 15.33 | ±1.11 | 17.76 | ±0.696 | 13.46 | ±1.31 |
| Proton | 34.80 | ±2.95 | 15.55 | ±1.65 | 17.77 | ±1.09 | 13.05 | ±1.30 |
| Iron | 34.65 | ±2.50 | 13.08 | ±0.930 | 15.64 | ±0.316 | 9.42 | ±0.543 |
| Carbon | 38.73 | ±3.36 | 14.38 | ±0.932 | 16.47 | ±0.380 | 10.51 | ±0.500 |

| **Deflection (mm)** | | | | | | |
|---|---|---|---|---|---|---|
| **Treatment** | **Elastic** | | **Maximum** | | **Fracture** | |
| Control | 0.516 | ±0.108 | 0.651 | ±0.087 | 1.01 | ±0.087 |
| Gamma | 0.464 | ±0.052 | 0.548 | ±0.028 | 0.799 | ±0.085 |
| Proton | 0.457 | ±0.049 | 0.555 | ±0.024 | 0.753 | ±0.086 |
| Iron | 0.396 | ±0.041 | 0.543 | ±0.025 | 1.01 | ±0.051 |
| Carbon | 0.397 | ±0.045 | 0.532 | ±0.020 | 0.941 | ±0.063 |

Values are listed as means ± standard error of the mean

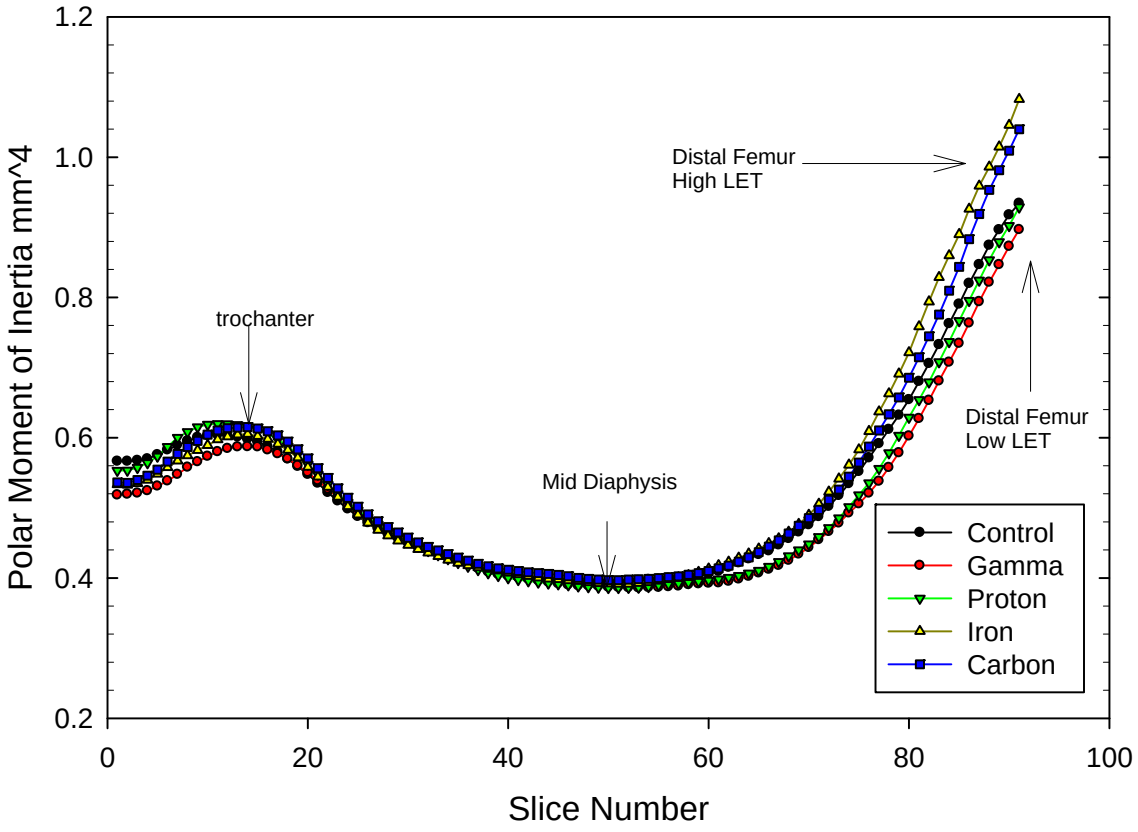


**Figure 3.2:** Polar moment of inertia per slice of all types for Multi-Type study. Slice 1 starts at the proximal portion of the diaphysis and continues down for approximately 9mm, to the distal end of the diaphysis. All the groups display together until the distal portion of the diaphysis is reached. A this portion a non significant grouping of the high-LET (Iron and Carbon) groups with a higher polar moment of inertia and the low-LET groups (gamma and proton) with a slightly decreased polar moment of inertia.

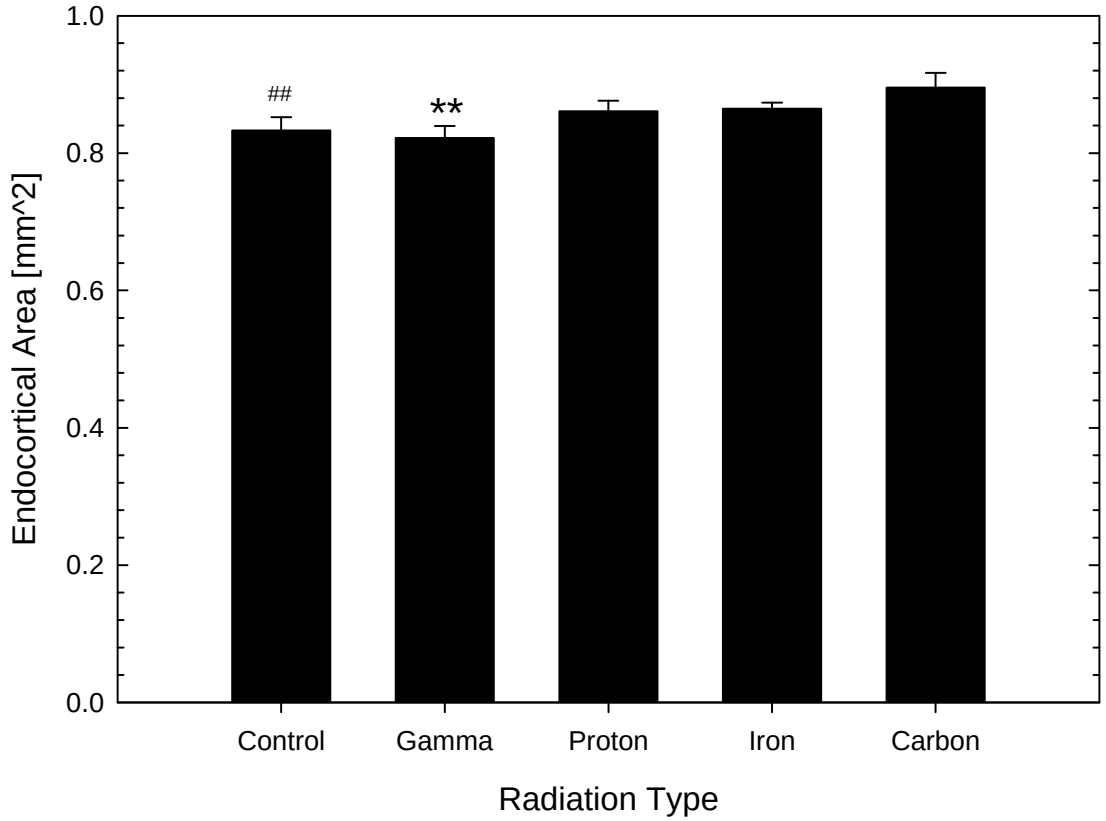


**Figure 3.3:** The endocortical area of the mid diaphysis of the femur for the Multi-Type study. The endocortical area of carbon is significantly increased when compared with gamma, P=0.033. A trend was seen between carbon and control groups with carbon having an increased endocortical, P=0.094 ** Denotes difference from Carbon and ## denotes a trend with Carbon. Error bars use standard error

**Table 3.2:** Quantitative histomorphometry and MicroCT from Multi-Type

| Treatment | Cortical Area ($mm^2$) | | Endo Cortical Area ($mm^2$) | | Micro Hardness | | Cortical Volume ($mm^3$) | | Mass (Kg) | |
|---|---|---|---|---|---|---|---|---|---|---|
| Control | 0.943 | ±0.0227 | 0.757 | ±0.0193 | 75.34 | ±2.047 | 9.468 | ±0.134 | 25.19 | ±0.410 |
| Gamma | 0.927 | ±0.0138 | 0.747 | ±0.0174 | 81.15 | ±1.681 | 9.305 | ±0.151 | 26.81 | ±0.800 |
| Proton | 0.911 | ±0.0175 | 0.775 | ±0.0154 | 76.50 | ±1.721 | 9.439 | ±0.0986 | 26.56 | ±0.916 |
| Iron | 0.928 | ±0.0127 | 0.778 | ±0.00901 | 74.39 | ±1.710 | 9.283 | ±0.127 | 26.76 | ±0.699 |
| Carbon | 0.905 | ±0.0131 | 0.806 | ±0.0216 | 75.10 | ±1.950 | 9.362 | ±0.0721 | 26.74 | ±0.442 |

Values are listed as means ± standard error of the mean

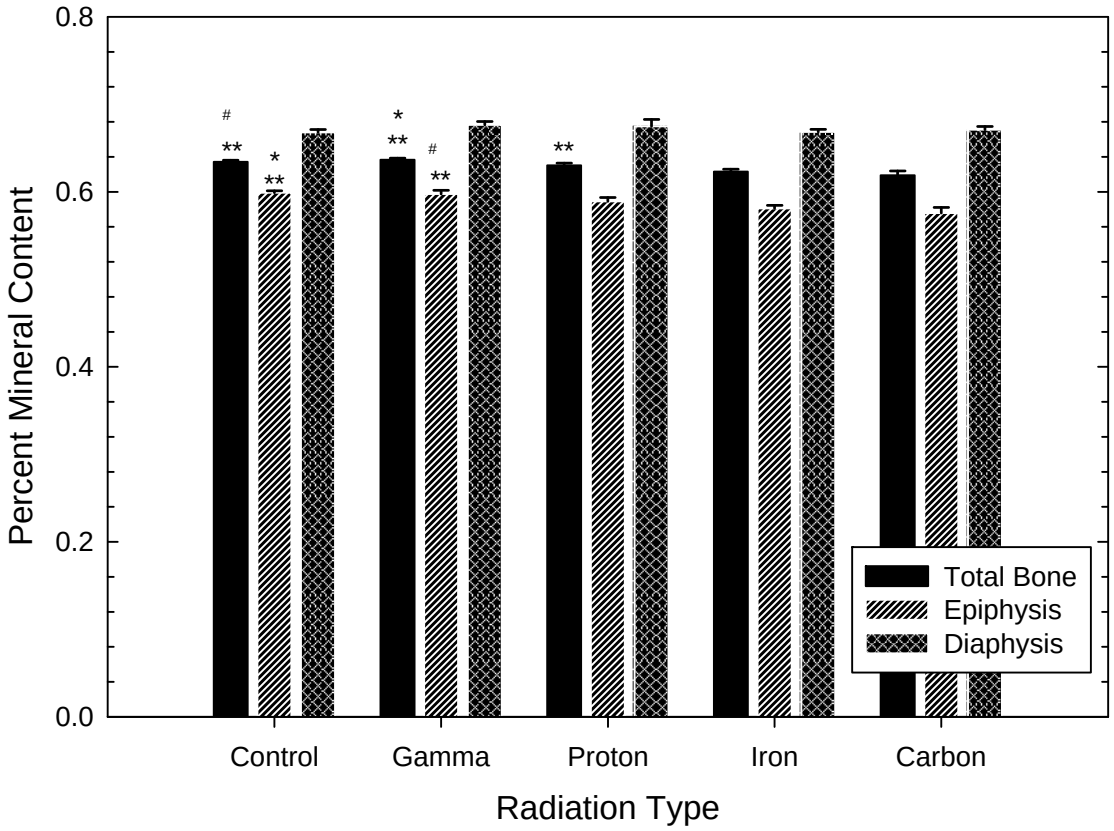


**Figure 3.4:** Percent mineral content of Multi-Type study, error bars using standard error of the mean. The epiphysis and diaphysis is broken up into individual bars with and additional bar for the whole femur. * Denotes significant difference from Iron, ** Denotes significant difference from Carbon, # Denotes trend with Iron.

### 3.3.1 High and Low-LET

Although cortical parameters were not significantly different from controls following irradiation, the ionizing density (LET) of the radian may have affected certain bone patterns. High-LET (carbon and iron) exposure may negatively affect some parameters to a greater extent than low-LET (gamma and proton). Following mechanical testing, fracture force of gamma irradiation increased when compared with the iron radiation group (Figure 3.5). Iron irradiation tended to decrease fracture force when compared to proton irradiation (Figure 3.5). Using microCT, the cortical porosity in mice

exposed to iron radiation was numerically increased compared to cortical porosity in mice exposed to proton and gamma radiation groups (Figure 3.6). Quantitative histomophometry revealed increased endocortical area in mice exposed to carbon radiation when compared with mice exposed to gamma radiation group (Figure 3.3). Results are shown in Table 3.

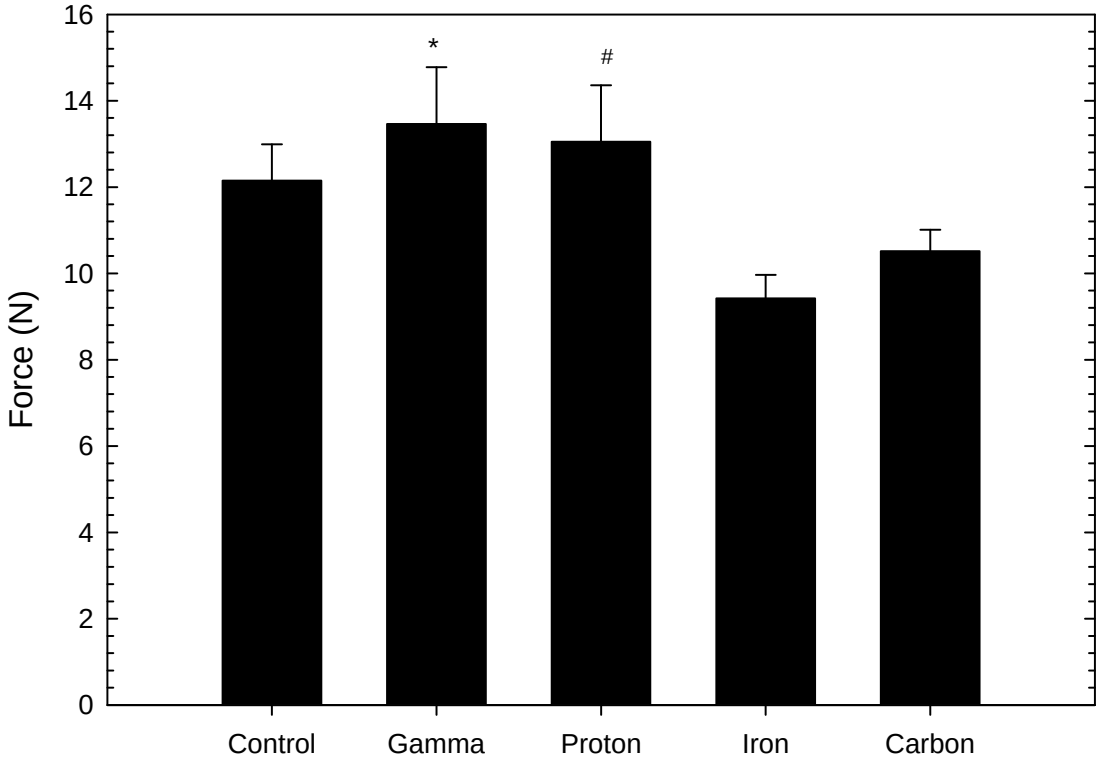


**Figure 3.5:** Fracture force of Multi-Type, Gamma was found to have a significantly greater fracture force than iron, P=0.034. Additionally, with the proton group a trend of a higher fracture force was seen when compared to iron, P=0.07. * Denotes difference from iron, error bars using standard error of the mean. # Denotes a trend from iron.

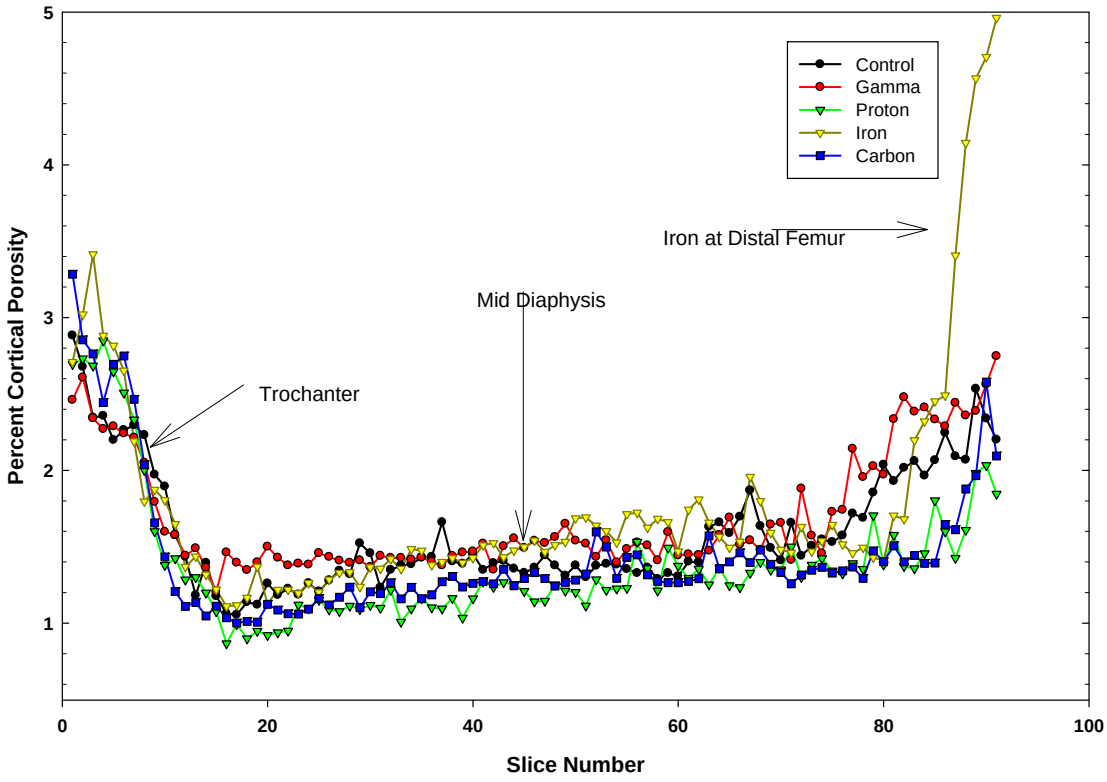


**Figure 3.6:** Cortical porosity per slice of all types in the Multi-Type study, slice one starts at the proximal end of the diaphysis and goes distally approximately 9mm. The plots for each appear to trend together until the distal portion of the diaphysis. At this section iron has a large peak in cortical porosity.

## 3.4 Discussion

### 3.4.1 Changes to Cortical Bone

Unlike trabecular bone (Hamilton et al., 2006b; Willey et al., Submitted 2007), there were remarkably few changes to cortical bone. No statistically different differences in cortical bone parameters were found between any of the radiation groups and controls for: mechanical properties (mechanical testing), structural properties (microCT, quantitative histomorphometry) or material properties (micro-hardness, percent mineral composition). However, an LET effect may exist. Heavy ion radiation (carbon and iron)

may reduce structural and mechanical strength when compared to low-LET (gamma and proton) radiation. Results obtained in this study seem to indicate that cortical bone is largely spared the devastating affects of radiation previously observed in trabecular bone in the proximal epiphysis of the tibia. However, this study was limited to diaphyseal cortical bone.

### 3.4.2 Difference in High and Low-LET

Despite the absence of statistically significant changes to cortical bone when the irradiated groups are compared to the control group, there were subtle change observed between high-LET (carbon and iron) and low-LET (gamma and proton) radiation. The comparison of the two LET types is difficult because relative to the control they are not significant but when compared to one another some difference appear. This illustrates a possible slight increase in one LET type with a small decrease in the other LET, although non significant against the control group. With microCT, the cortical porosity of the group treated with iron radiation was significantly greater than both the proton and gamma groups indicating an increased resorption specifically at proximal and distal portions of the diaphysis. This increased in porosity would reduce structural and mechanical strength.

For mechanical testing, the fracture force of the gamma irradiated group was significantly greater compared to the iron irradiated group. Quantitative histomophometry revealed increase endocortical area in the bones of iron irradiated mice when compared to bones from mice exposed to gamma radiation. This finding suggests expansion of the marrow cavity without compensatory expansion of the periosteal area to maintain the average cortical area and should result in a net loss of structural strength.

The cross sectional area of the cortical bone must increase to successfully structurally carry the same loads applied with an increase in trabecular resorption which was observed in the prior study.

The distal portion of the Multi-Type femora is shown to have an increase in porosity (Figure 3.6) and area, demonstrating a possible LET effect. Polar moment of inertia shows a visual but insignificant increase with the High-LET groups (Figure 3.2). These all correspond to one another exceptionally well. With an increase in area at the distal section the inertia would also increase. This increase is not followed by a difference in cortical area or an increase in periosteal area; however, in a few instances there is an LET difference resulting in an increase in the endocortical area. Changes in these regions, though, could possibly be significant with a larger sample size. This visual increase in inertia and in porosity at this region should ultimately result in reduced strength; nevertheless, it is difficult to mechanically test the distal portion of the femur of a mouse bone because of the small size of the bones and difficulty properly loading femoral heads.

As formerly reported, there was a greater decrease in trabecular thickness following exposure to high-LET radiation (Hamilton et al., 2006b). Similar LET effects are observed on cortical bone, suggesting a more negative effect of heavy ions on bone strength. Though, these changes are subtle compared to the large decline in trabecular bone of all radiation types. In spaceflight, cortical bone as well as trabecular bone is remodeled, but there is a proportionately larger quantity of trabecular bone lost (Lang et al., 2004). The results of bone loss experienced in microgravity are an increased risk of bone fracture during and after missions (Lang et al., 2006).

### 3.4.3 Trabecular Specificity

This study leads us to ponder why radiation more severely damages trabecular bone. Literature identifies negative effects of radiation on cortical bone strength, but at doses far higher than experienced in spaceflight. The specificity of radiation damaging trabecular bone preferentially over cortical bone at lower/moderate doses, with few to no effects on cortical bone, is particularly interesting. A unique property of trabecular bone is a proportionally increased surface area compared to cortical bone, leading to a greater direct contact with bone marrow. Trabecular bone is spatially contained within the metabolically active red marrow at the epiphyses of long bones and vertebrae. Bone loss observed at lower/moderate doses is somewhat surprising, because of bone's insensitivity to radiation, with a tissue weighting factor of 0.01. Bone marrow, on the other hand, is far more radiation sensitive with a tissue weighing factor of 0.12 (International Commission on Radiological Protection., 1992).

A possible explanation for the increased loss of trabecular bone is this proximity to marrow and the marrow's increased activity immediately following irradiation (International Commission on Radiological Protection., 1992). Greater material density of bone (Apparent Bone Density 1.85 g/cm3) (Bilezikian et al., 1996) may cause more ionizing by interactions with the larger atoms of calcium and phosphorus. This is because of the relative paucity of cells within bone and the level of cell maturity as osteocytes are terminally differentiated, non dividing cells. Thus possibly, the ionization possibly has little biological effect within compact bone, where the interface of bone and bone marrow has a greater potential for change and an increased ionization.

At the interface of bone marrow, an ionizing event within bone may impact marrow close to the bone surface. This ionizing amplification at the interface of bone and marrow may cause more damage leading to an inflammatory response that result in a non-specific activation of osteoclasts (bone specific macrophages). Willey et al. hypothesized that osteoclast activation is initiated by an inflammatory response (Willey et al., Submitted 2007), not dissimilar to bone loss associated with rheumatoid arthritis (Findlay and Haynes, 2005), and wear debris osteolysis (Holding et al., 2006). Lorimore et al (Lorimore and Wright, 2003) identified a clear inflammatory response to damaged marrow. However, cortical bone has only one surface exposed to marrow and is not fully immersed in the marrow's reaction to radiation. Ionizing amplification may also occur at the cortical bone and marrow interface, but the size of the affect on marrow may be far less due to spatial orientation.

### 3.4.4 Limitations

There were several limitations to the evaluations in the Multi-Type study. Maeda et al. (Maeda et al., 1988) showed the effects of a very high acute dose of radiation were not seen in the cortical bone until 10 weeks post-irradiation, in rats. However, in this study, tests such as percent mineral composition and micro-hardness indentation should indicate material changes if the bone was remodeling. The cortical bone of mice is not vascularized in the same manner as larger animals with haversian canals. Cortical bone in these smaller animals may respond differently to radiation than cortical bone with haversian canals. Increased surface area provided by vasculature in haversian bone may more resemble trabecular bone responses with increased resorption. Moreover, radiation damages vasculature (Mitchell and Logan, 1998) and may initiate a larger bone response

due to widespread inflammation in damaged blood vessels. Increase vascularity within the cortical bone allows the possibility of increased ionization and resulting increased resorption. Lack of study control, limited time points evaluated, and decrease vascularity all were limitations to the Multi-Type study.

### 3.4.5 Implications

In this study, radiation had no statistically significant affect on cortical bone in comparison between irradiated and non-irradiated mice. The effects of radiation on cortical bone were shown to have no difference between the irradiated and non-irradiated animals. However, cortical bone may still be affected in humans and animals with haversian bone. Testing in larger animals with haversian bone is necessary to evaluate the impact of increased porosity and blood supply within the cortical bone. Additional analyses of cortical parameters in the neck of the femur, the location of the majority of hip fractures in trabecular bone deficient osteoporosis, may provide additional insight into the anatomic and functional consequences of irradiation. Changes in the time from exposure to examination should also be assessed to more accurately establish the physiological response. Despite its limitation, when combined with results of previous work, this study demonstrates great variation in the affects of radiation on different structural components in bone.

## 3.5 References:


Benton, E. R. and E. V. Benton (2001). "Space radiation dosimetry in low-Earth orbit and beyond." Nucl Instrum Methods Phys Res B **184**(1-2): 255-94.

Bilezikian, J. P., L. G. Raisz, et al. (1996). Principles of bone biology. San Diego, Academic Press.

Blakely, E. A. (2000). "Biological effects of cosmic radiation: deterministic and stochastic." Health Phys **79**(5): 495-506.

Broz, J. J., S. J. Simske, et al. (1993). "Effects of rehydration state on the flexural properties of whole mouse long bones." J Biomech Eng **115**(4A): 447-9.

Callister, W. D. (2007). Materials science and engineering : an introduction. New York, John Wiley & Sons.

Epelman, S. and D. R. Hamilton (2006). "Medical mitigation strategies for acute radiation exposure during spaceflight." Aviat Space Environ Med **77**(2): 130-9.

Findlay, D. M. and D. R. Haynes (2005). "Mechanisms of bone loss in rheumatoid arthritis." Mod Rheumatol **15**(4): 232-40.

Foullon, C., Andrew Holmes-Siedle, Norma Bock Crosby, Daniel Heynderickx (2004). "Radiation Exposure and Mission Strategies for Interplanetary Manned Mission." (REMSIM technical Note 5) Alenia Spazio Technical Note.

Goodship, A. E., J. L. Cunningham, et al. (1998). "Bone loss during long term space flight is prevented by the application of a short term impulsive mechanical stimulus." Acta Astronaut **43**(3-6): 65-75.

Gridley, D. S., M. J. Pecaut, et al. (2002). "Dose and dose rate effects of whole-body proton irradiation on leukocyte populations and lymphoid organs: part I." Immunol Lett **80**(1): 55-66.

Hamilton, S. A., M. J. Pecaut, et al. (2006). "A Murine Model for Bone Loss from Therapeutic and Space-Relevant Sources of Radiation." J Appl Physiol.

Hamilton, S. A., M. J. Pecaut, et al. (2006). "A murine model for bone loss from therapeutic and space-relevant sources of radiation." J Appl Physiol **101**(3): 789-93.

Heilbron, L., T. Nakamura, et al. (2005). "Overview of secondary neutron production relevant to shielding in space." Radiat Prot Dosimetry **116**(1-4 Pt 2): 140-3.

Holding, C. A., D. M. Findlay, et al. (2006). "The correlation of RANK, RANKL and TNFalpha expression with bone loss volume and polyethylene wear debris around hip implants." Biomaterials **27**(30): 5212-9.

Homminga, J., H. Weinans, et al. (2001). "Osteoporosis changes the amount of vertebral trabecular bone at risk of fracture but not the vertebral load distribution." Spine **26**(14): 1555-61.

International Commission on Radiological Protection. (1992). 1990 recommendations of the International Commission on Radiological Protection : user's edition. Oxford ; New York, :Published for the International Commission on Radiological Protection by Pergamon Press.

Ito, M., A. Nishida, et al. (2002). "Contribution of trabecular and cortical components to the mechanical properties of bone and their regulating parameters." Bone **31**(3): 351-8.

Lang, T., A. LeBlanc, et al. (2004). "Cortical and trabecular bone mineral loss from the spine and hip in long-duration spaceflight." J Bone Miner Res **19**(6): 1006-12.

Lang, T. F., A. D. Leblanc, et al. (2006). "Adaptation of the proximal femur to skeletal reloading after long-duration spaceflight." J Bone Miner Res **21**(8): 1224-30.

Lorimore, S. A. and E. G. Wright (2003). "Radiation-induced genomic instability and bystander effects: related inflammatory-type responses to radiation-induced stress and injury? A review." Int J Radiat Biol **79**(1): 15-25.

Maeda, M., M. H. Bryant, et al. (1988). "Effects of irradiation on cortical bone and their time-related changes. A biomechanical and histomorphological study." J Bone Joint Surg Am **70**(3): 392-9.

Moore, F. D. (1992). "Radiation burdens for humans on prolonged exomagnetospheric voyages." Faseb J **6**(6): 2338-43.

Nyaruba, M. M., I. Yamamoto, et al. (1998). "Bone fragility induced by X-ray irradiation in relation to cortical bone-mineral content." Acta Radiol **39**(1): 43-6.

Parsons, J. L. and L. W. Townsend (2000). "Interplanetary crew dose rates for the August 1972 solar particle event." Radiat Res **153**(6): 729-33.

Pecaut, M. J., A. L. Smith, et al. (2000). "Modification of immunologic and hematologic variables by method of CO2 euthanasia." Comp Med **50**(6): 595-602.

Rohrer, M. D., Y. Kim, et al. (1979). "The effect of cobalt-60 irradiation on monkey mandibles." Oral Surg Oral Med Oral Pathol **48**(5): 424-40.

Simonsen, L. C., F. A. Cucinotta, et al. (1993). "Temporal analysis of the October 1989 proton flare using computerized anatomical models." Radiat Res **133**(1): 1-11.

Smith, S. M., M. E. Wastney, et al. (1999). "Calcium metabolism before, during, and after a 3-mo spaceflight: kinetic and biochemical changes." Am J Physiol **277**(1 Pt 2): R1-10.

Stephens, D. L., Jr., L. W. Townsend, et al. (2005). "Interplanetary crew dose estimates for worst case solar particle events based on historical data for the Carrington flare of 1859." Acta Astronaut **56**(9-12): 969-74.

Sugimoto, M., S. Takahashi, et al. (1991). "Changes in bone after high-dose irradiation. Biomechanics and histomorphology." J Bone Joint Surg Br **73**(3): 492-7.

Tilton, F. E., J. J. Degioanni, et al. (1980). "Long-term follow-up of Skylab bone demineralization." Aviat Space Environ Med **51**(11): 1209-13.

Townsend, L. W. (2005). "Implications of the space radiation environment for human exploration in deep space." Radiat Prot Dosimetry **115**(1-4): 44-50.

Vico, L., P. Collet, et al. (2000). "Effects of long-term microgravity exposure on cancellous and cortical weight-bearing bones of cosmonauts." Lancet **355**(9215): 1607-11.

# CHAPTER 4

# EFFECTS TO DIAPHYSEAL CORTICAL BONE AFTER 7 GRAY RADIATION

## 4.1 Introduction

Two recent, articles identified increased fracture rates (Baxter et al., 2005) and joint replacement (Oeffinger et al., 2006) caused by osteoporosis in cancer survivors receiving radiation therapy. The previous studies by Hamilton et al and Willey et al. observed a rapid decline in trabecular volume fraction (29-39% and 54% respectively) two weeks following high dose irradiation (Hamilton et al., 2006b; Willey et al., Submitted 2007). About half of cancer patients will receive radiation therapy at some point during treatment (Bentzen, 2006). Cancer patients are typically older (65 years old or older) and are predisposed to osteoporosis. The purpose of this chapter is to evaluate a mouse study designed to evaluate radiation exposure typical of therapeutic applications and report skeletal changes specific to cortical bone. An applicable link to spaceflight does not fully exist for this type of exposure. In is unlikely that astronauts in space would be exposed to as much as 7 Gy and the primary source would be from protons and not gamma radiation.

### 4.1.1 Clinical Application

Roughly 1.4 million people developed new cases of cancer in 2006, and approximately 50% of these patients were treated with radiation during the course of the disease (Bentzen, 2006). Radiation therapy is an important tool in improving cancer survival rates; an estimated five-year survival rate for breast, colon, and prostate cancer

are 88.2%, 64.1%, and 99.8% respectively (American Cancer Society, 2006). However, radiation treatment has side effects and limitations requiring better understanding, particularly as it relates to inflammation (Bentzen, 2006). These side effects include the deleterious outcomes on bone creating an increased fracture risk (Baxter et al., 2005; Hamilton et al., 2006b; Maeda et al., 1988; Mitchell and Logan, 1998; Nyaruba et al., 1998; Sugimoto et al., 1991). Depending on the cancer treatment, patients may receive daily fractional doses of 1.8-2 Gray (Gy) with cumulative doses of 40-50 Gy (generally x-rays and electrons, with protons used less commonly) local to tumor (Bolek et al., 1996). Treatment of bone pain associated with metastatic tumors has recently included single high doses of up to 8 Gy local to the tumor (Hartsell et al., 2005). For pelvic and bone cancers (Baxter et al., 2005; Sze et al., 2003) increased fracture rates are reported (Baxter et al., 2005; Rex and Elsworth, 1998).

## 4.2 Methods and Materials

### 4.2.1 High-Dose Irradiation

The study was conducted using nine-week old female C57BL/6 mice (Charles River Breeding Labs, Wilmington, MA). Animals were acclimatized for one week prior to irradiation, with food and water available ad libitum. The study was conducted with the approval of the Institutional Animal Care and Use Committee of Loma Linda.

Prior to radiation, the animals were placed into individual rectangular polystyrene boxes with air holes (30 mm x 30 mm x 85 mm) (Gridley et al., 2002). A group of mice (n=6) received whole-body irradiation from a 60-Cobalt ($^{60}$Co) gamma ray linear energy transfer (Vico et al.) = 0.23 keV/micron, n=6. For $^{60}$Co irradiation, a horizontal beam from a retired AECL (Atomic Energy of Canada, Ltd.; Commercial Products Division;

Ottawa, Canada) Eldorado therapy unit was used. A single dose of 7 Gy was delivered to the animals. The control group (n=6) was not irradiated. Animals were then sacrificed 14 days after exposure.

### 4.2.2 High-Dose Assays

4.2.2.1 Mechanical Testing: Femora in the High-Dose study were biomechanically tested. Bones were soaked in sodium chloride for 1.5 hours prior to testing (Broz et al., 1993). A three-point bending test (Figure 4.1) examined mechanical properties of the femora at the mid-diaphysis using an Instron 5582 (Instron Corporation, Norwood, MA), with a 50 N load cell (0.05 N resolution) and Bluehill 2 (Instron Corporation, Norwood, MA) software. Femora were loaded to failure using an anvil with a 9 mm span length. The femur was placed with condyles facing upward in the Instron with a deflection rate of 5 mm/min. Force (N) and deflection (Homminga et al.) were collected at 10 Hz. A custom written software program was used to determine the elastic limit ($P_e$), maximum force ($P_m$) and force at fracture ($P_f$) from the measured values. Stiffness (S) analyzed from obtained force deflection curves

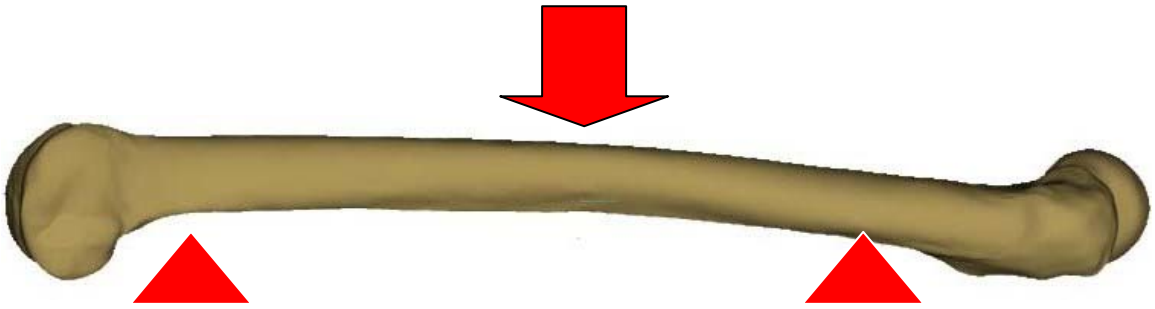

**Figure 4.1:** Illustration of a three point bending technique used in the mechanical testing of these femora. The bone is in the correct anatomical position for testing. (http://biomech.me.unr.edu/hip.htm)

4.2.2.2 Micro-computed Tomography Properties: Femora were removed and cleaned of non-osseous tissue to prepare them for micro-computed tomography (microCT) analysis (*microCT20*, Scanco Medical AG, Bassersdorf, Switzerland). Bones were analyzed to determine maximum, minimum and polar moments of inertia, cortical porosity and cortical volume. One hundred and five slices of the diaphysis were scanned (the span of the diaphysis that was mechanically tested), with each slice having a thickness of 9 microns and 100 microns between slices. Scans were initiated at the base of the femoral neck and sequentially analyzed to isolate the junction of the femoral neck and diaphysis. A total of 91 slices (approximately 9mm) were evaluated distal to this established reference point. Parameters were examined to evaluate the ability of the cortical bone to maintain structure following irradiation.

4.2.2.3 Quantitative Histomorphometry: After removal of non-osseous tissue, the femora used in this study were placed in neutral buffered 10% formalin for 48 hours followed by immersion in 70% ethanol. The bones were dried for two days prior to embedding. Femora measured from the ball at the proximal femoral head to the distal end of the condyles. Bones were embedded in Non-infiltrating Epo-Kwick epoxy (Buehler Ltd., Lake Bluff, IL) and allowed to dry for 24 hours prior to cutting. Femora were cut distally to the third trochanter (Buehler, 12.7 cm x 0.5 cm diamond blade). Disks sections were polished using 600, 800, and 1200 grit carbide paper and diamond paste. The femora were viewed on a Zeiss Axioskop 2 plus microscope (Carl Zeiss MicroImaging, Inc., Thornwood, NY) with AxioVision software for digital imaging. SigmaScan Pro 5 (Systat Software, Inc., Point Richmond, CA) software was used to analyze digital images of the

specimens. Individual bones were viewed at 5X magnification under UV light using an Fs 05 filter. The major and minor axis diameters were computed using the software. The perimeter of the endocortical (Ec.Pm) and periosteal (Ps.Pm) surfaces were traced and analyzed for area (Ec.Ar, Ps.Ar) and length (Figure 4.2). Cortical area was calculated by subtracting the endocortical areas from the periosteal area (Ct.Ar = Ps.Ar. – Ec.Ar).

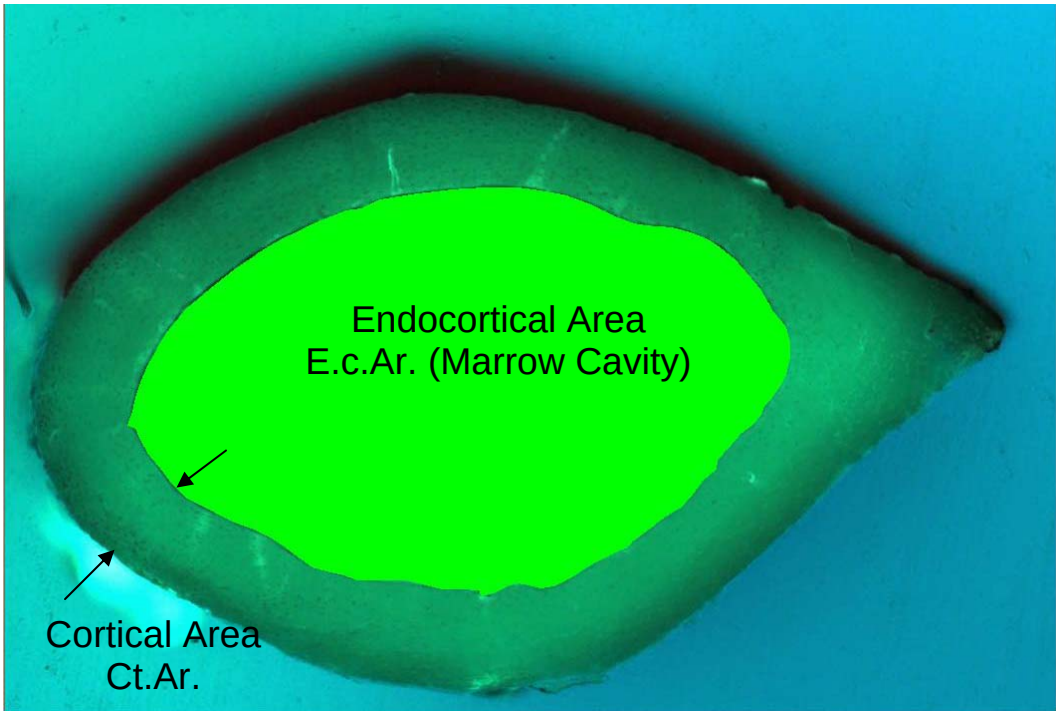


**Figure 4.2:** Cross sectional view of femur with markings for quantitative histomorphometry evaluation of the femur. This section is just distal to the third trochanter.

4.2.2.4 Compositional Analysis: Femora in the High-Dose studies were examined for mineral composition. The bones were ashed using an Isotemp Muffle furnace (Fisher Scientific Company L.L.C., Pittsburgh, PA) to assess mineral composition within each bone. Proximal and distal epiphyses were separated from the diaphysis and weights

recorded. Each component was then positioned in the oven at 105$^{o}$C for 24 hours and weights were again recorded (dry mass, Dry-M). Bones were baked at 800$^{o}$C for 24 hours and reweighed (mineral mass, Min-M). Organic mass (Org-M) was calculated as the difference between dry mass and mineral mass (Org-M = Dry-M – Min-M). The percent mineral content was calculated as by Min-M/Dry-M*100%.

4.2.2.5 Micro-Hardness Indention: The same femoral bone disks used for quantitative histomorphometry were used for the micro-hardness indentation test. Bones were then analyzed using a Buehler Maicromet 5101 micro-hardness indenter (Buehler, Lake Bluff, IL). The indentions were performed on the lateral side of each bone. Four indentions were made with a 40 μm spacing from the periosteal surface and between each indention. The length and width of each indention was measured and recorded at tips of the indention, d1 and d2 (Figure 4.3). An average was then computed for the micro-hardness value for each bone. Vicker's method was used to calculate the hardness of each bone (Callister, 2007) and to compare them to the control. This method adjusts for the ocular magnification at measurement uses an average of the lengths and widths of the diamond shaped indentions.

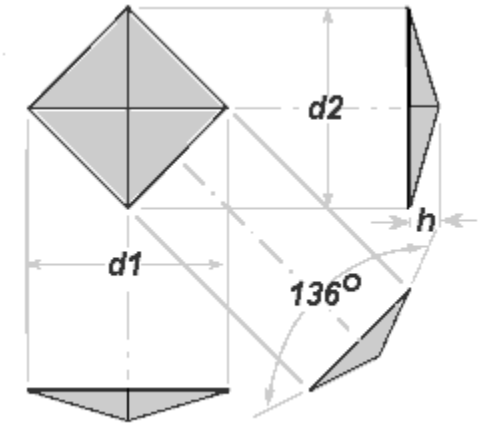


**Figure 4.3:** Illustration of the indention made from the micro-hardness indenter. The d1 and d2 dimensions were used with the Vicker's hardness method to establish a hardness value of the bone (Richard E. Thacker, 2004).

4.2.2.6 Statistics: Statistical analyses were performed using SigmaStat software version 2.03 (Systat Software Inc., Richmond, California). Statistical comparisons were performed using a one-way ANOVA with a Tukey's HSD follow up test. Alpha was set at 0.05, $\alpha = 0.05$. The primary goal of statistics was to compare the irradiated groups to the control groups. Subsequently, the Tukey's follow-up test compares all groups to one another and differences between each group can be observed.

## 4.3 Results

### 4.3.1 High-Dose

In this High-Dose study groups differed significantly in the percent mineral content of the femoral diaphysis (Figure 4.4) and in animal mass (Figure 4.5). No significant differences were identified in mechanical testing (Table 4.1, Figure 4.5), microCT (Table

4.2, Figure 4.7 and Figure 4.8), quantitative histomophometry (Table 4.2), micro hardness (Table 4.2) or bone length.

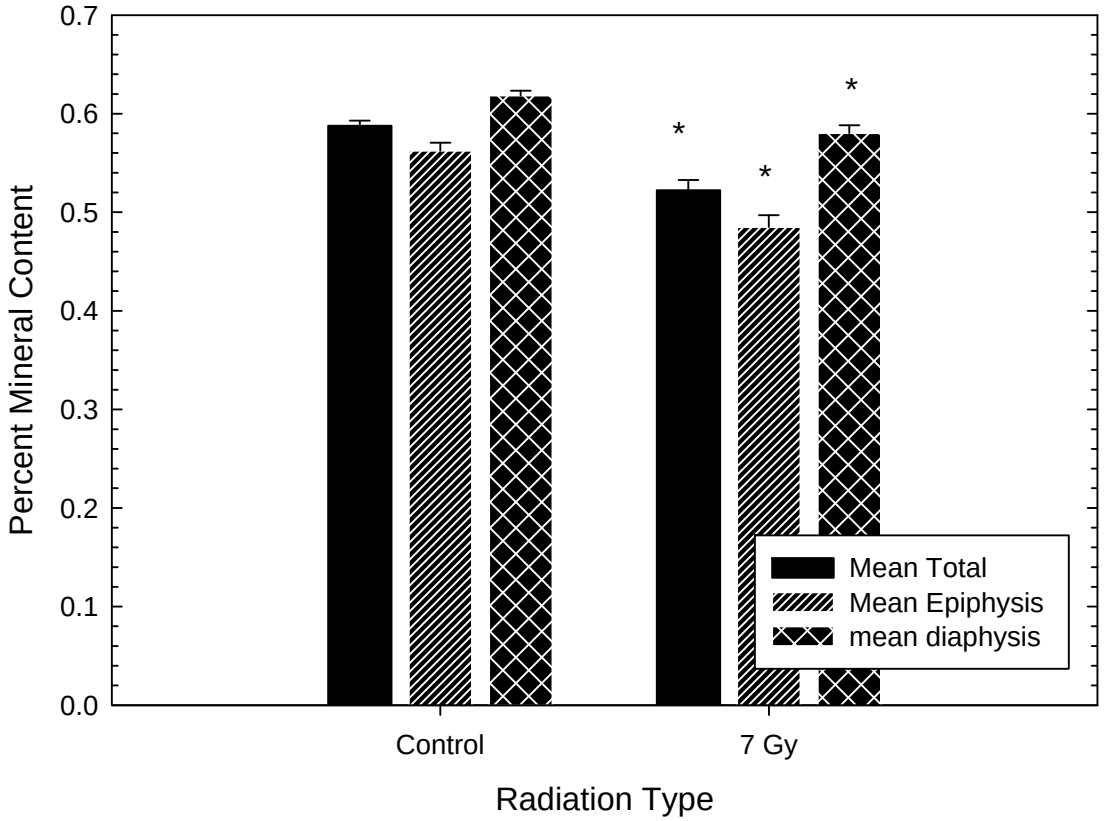


**Figure 4.4:** Percent mineral content of High-Dose femora, error bars using standard error of the mean. * Denotes statistically significant difference from control. All parts of the irradiated group are different from the control group.

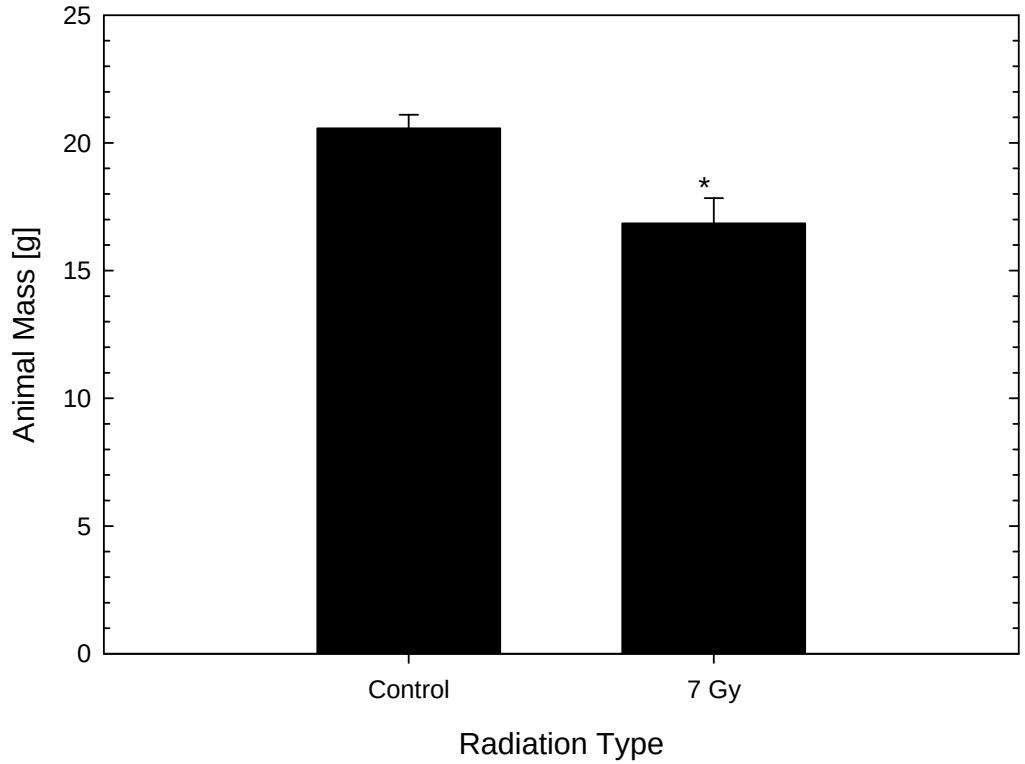


**Figure 4.5:** The animal mass of the High-Dose study. Note the animal mass of the irradiated group is statistically significantly different from the control group. The error bars are using standard error of the mean.

**Table 4.1:** Mechanical testing data from High-Dose study.

| Treatment | Stiffness (N/mm) | Force (N) | | |
|---|---|---|---|---|
| | | Elastic | Maximum | Fracture |
| Control | 37.99 ±1.48 | 9.86 ±0.271 | 12.43 ±0.354 | 7.52 ±0.918 |
| 7 Gy | 38.68 ±2.16 | 9.99 ±0.277 | 12.40 ±0.294 | 8.11 ±0.785 |

| Treatment | Deflection (mm) | | |
|---|---|---|---|
| | Elastic | Maximum | Fracture |
| Control | 0.260 ±0.011 | 0.397 ±0.021 | 0.798 ±0.164 |
| 7 Gy | 0.260 ±0.010 | 0.418 ±0.043 | 0.816 ±0.101 |

Values are listed as means ± standard error of the mean

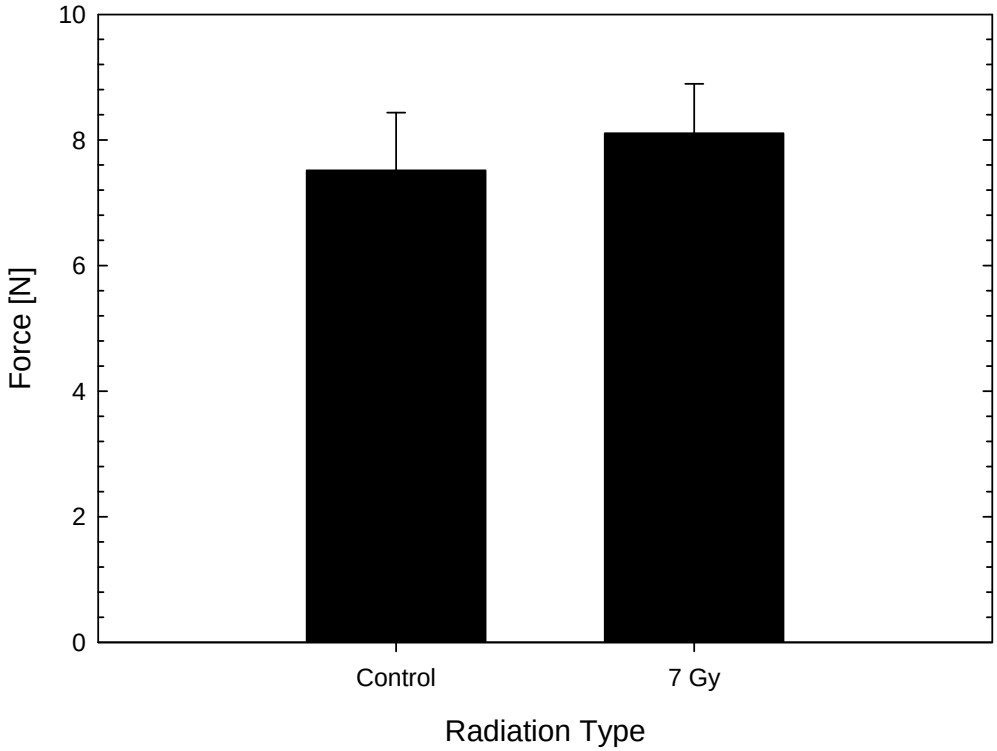


**Figure 4.6:** Fracture Force of High-Dose bones, error bars using standard error of the mean

**Table 4.2:** Quantitative Histomophometry, Micro Hardness and MicroCT from High-Dose study

| Treatment | Cortical Area ($mm^2$) | Endo Cortical Area ($mm^2$) | Micro Hardness Indention | Cortical Volume ($mm^3$) |
|---|---|---|---|---|
| Control | 0.698 $\pm$0.0142 | 0.974 $\pm$0.0194 | 49.1 $\pm$1.42 | 7.75 $\pm$0.104 |
| 7 Gy Gamma | 0.695 $\pm$0.00462 | 0.966 $\pm$0.0132 | 49.3 $\pm$2.25 | 7.93 $\pm$0.119 |

Values are listed as means $\pm$ error using standard error of the mean

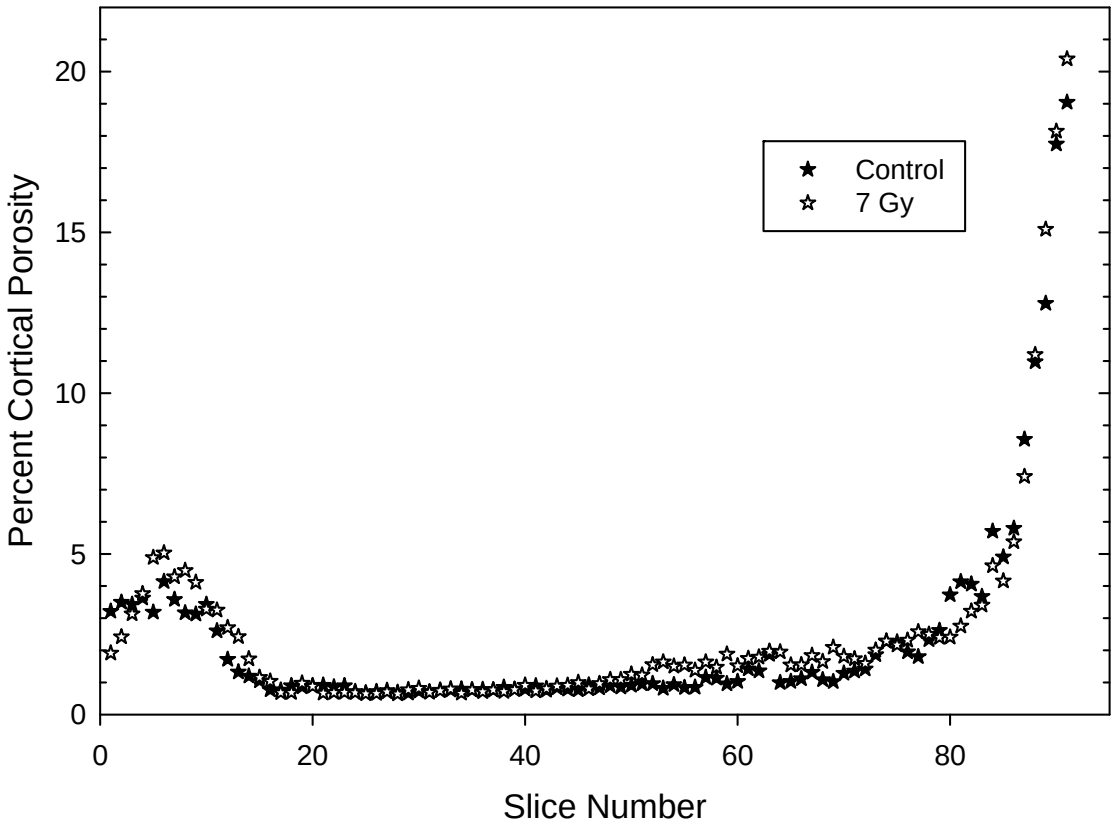


**Figure 4.7:** Cortical porosity of the femora diaphysis on a per slice basis for High-Dose study. The porosity was found on a per slice basis starting at the proximal diaphysis and continuing 9 mm to the distal diaphysis. The two graphs follow one another closely.

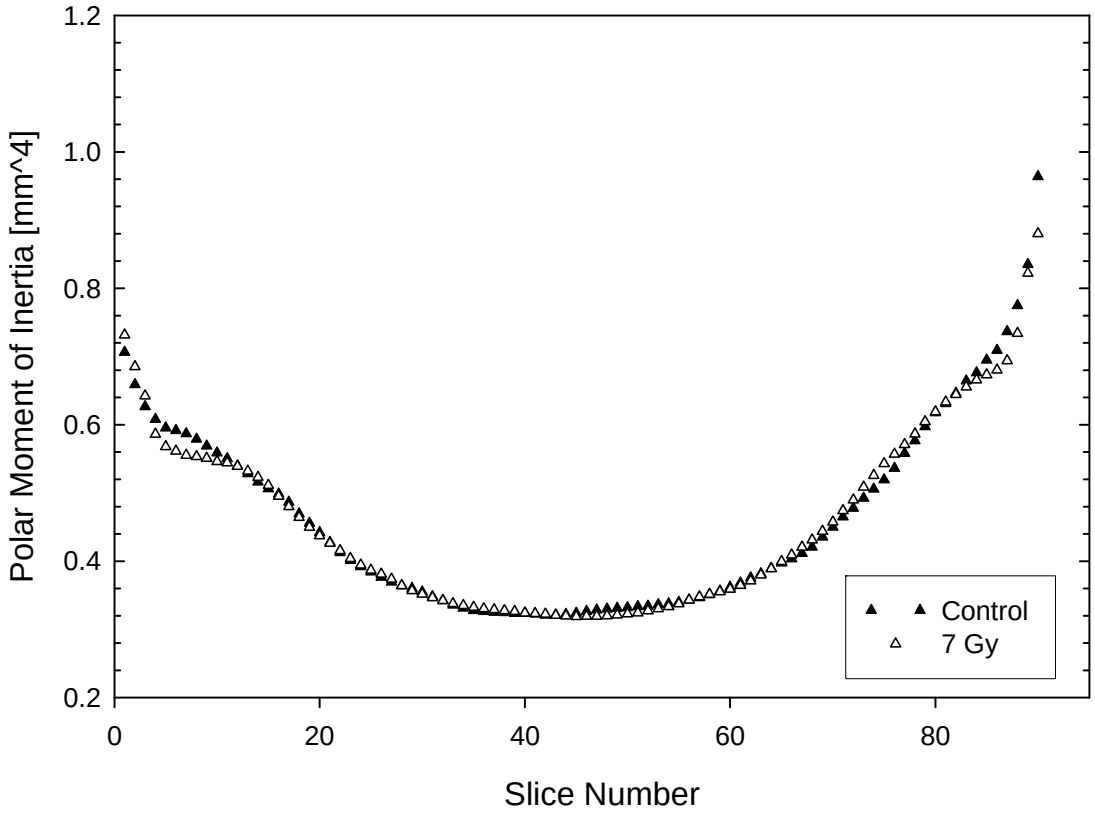


**Figure 4.8:** Polar moment of inertia for the High-Dose study. This is performed on a per slice basis. Zero starts at the proximal diaphysis and continues down 9 mm to the distal diaphysis. Notice the two groups follow together well and match the overall shape of the Multi-Type polar moment of inertia graph.

## 4.4 Discussion

### 4.4.1 Few Changes in Cortical Bone

Similar to the Multi-Type study, there were remarkably few cortical bone changes in this High-Dose study. The High-Dose group did demonstrate a significant decrease in percent mineral composition in bones from irradiated mice, suggesting increased bone resorption during this short experiment. However, in the absence of changes in micro-hardness and mechanical stiffness, we believe this may be a result of including some trabecular bone in the diaphysis section. This is seen in Figure 4.9 where trabecular bone is clearly evident in the distal end of these femora.

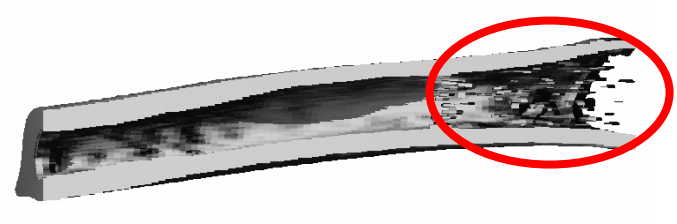

**Figure 4.9:** A microCT cut away view of the diaphyseal region of the femur. This is a femur from the High-Dose study, a control bone. The left end of the bone is proximal, while the right end is the distal portion. Within the red circle trabecular bone can be seen.

### 4.4.2 Trabecular versus Cortical Loss in Pathological Diseases

The differential response between trabecular and cortical bone suggests that radiation has site-specific effects on bone that occurs within a range of doses (2 – 7 Gy). For many diseases bone loss is greater in trabecular bone but not limited to this specific type of bone. Trabecular bone has a greater surface area which leads to an increased aptitude for remodeling (Seeman and Delmas, 2006). Examples of this phenomenon are spaceflight (Lang et al., 2004), type I osteoporosis (Lamichhane, 2005), early metastatic cancer (Coleman, 1997) and glucocorticoid induced osteoporosis (de Gregorio et al., 2006). Trabecular bone was also evaluated in the vertebrae after radiation therapy and a decline in bone mineral content was found 5 weeks post-irradiation (Kinji Nishiyama, 1992).

Age related, or senile/type II, osteoporosis is an example of a pathological process that effects cortical and trabecular bone equally (Lamichhane, 2005). Type II osteoporosis results in cortical thinning and an increased cross-sectional diameter of the diaphyseal portion of long bones. It is distinctive in that it may take many years to manifest measurable declines in bone density and strength. Pathological bone disease

often affects trabecular bone to a greater degree than cortical bone, but not with the differential magnitude observed following radiation exposure.

### 4.4.3 Immune Response

Radiation has an effect on the immune cells and its interaction with bone. The T-cell in inflammation causes osteoclastogenesis and osteoclast recruitment (Kong et al., 1999). Radiation is known to generate reactive oxygen species (ROS) which causes an inflammatory tissue response (Van der Meeren et al., 2003). ROS can initiate bone loss through mediation of osteoclastic and osteoblastic activity. The life span of the osteoclast is increased by ROS providing additional time for bone resorption (Ha et al., 2004). ROS can induce differentiation of osteoclastic precursor cells and activate existing osteoclast recruitment (Hall et al., 1995; Steinbeck et al., 1998). Bone formation is also inhibited as a result of ROS formation (Bai et al., 2004; Mody et al., 2001). Additionally, ROS can cause osteocyte apoptosis (Kikuyama et al., 2002) which is believed to regulator in bone micro-crack remodeling (Noble, 2005). Radiation-induced inflammation compounded by possible ionization amplification and ROS generation seem likely mechanisms to explain the accelerated bone loss following irradiation.

### 4.4.4 Negative effects in Cortical Bone

Literature indicates that a large single dose of radiation reduce cortical bone strength (Sugimoto et al., 1991). This would not be typical of radiation therapy where small doses are administered once or twice daily for several weeks to reach a cumulative exposure high enough to kill tumor cells. Once daily fracture have reduced strength of cortical but not to the magnitude of the large single dose and twice daily fractionated

doses do not significantly reduce cortical bone strength as severely as a single dose (Nyaruba et al., 1998). Many of the studies performed administer higher doses to obtain physiological effects but are not clinically relevant. Several weeks after radiation exposure may be required to allow sufficient cortical bone remodeling to demonstrate reductions in bone strength. The doses used in our studies were comparable to those used in single treatment radiotherapy or what would be a cumulative dose in space in the absence of a solar particle event without adequate shielding. A 7 Gy dose would be a high exposure in radiotherapy and unlikely in spaceflight. Cortical bone can be damaged by radiation exposure, but the exposure might have to be a large dose of low-LET or a high-LET type.

# CHAPTER 5

# CONCLUSIONS AND RECOMMENDATIONS

Data was presented from studies that characterize the effects of radiation on the mechanical, structural and material properties of diaphyseal cortical bone of mice. These two studies represented the extremes in both dose (lower/moderate 2 Gy and higher 7 Gy) and time following exposure (4 months and 2 weeks, respectively). These data provides fundamental information to guide future studies on radiation and cortical bone attributes. In general, cortical bone is resistant to radiation-induced bone loss, compared to the large loss of trabecular bone previously characterized. High-LET radiation (carbon and iron) appears to have a greater negative effect on cortical bone compared to low-LET radiation (gamma and proton) though the differences are subtle when compared to the more demonstrable changes observed in trabecular bone.

Cortical bone is not significantly depleted by the differentiation of radiation types or change in dose magnitude, when compared to non-irradiated control mice. There were, however, losses in trabecular bone, trabecular volume fraction, and connectivity in the study involving the Multi-Type radiation study mice (Hamilton et al., 2006b). The trabecular thickness was affected when exposed to high-LET doses which was supported by the data in the previous Multi-Type study examination (Hamilton et al., 2006b). Changes in cortical bone were possibly absent because of the selected doses and time points used with these two studies. However, there was an LET effect observed when comparing high-LET and low-LET radiation types. This could potentially suggest that the high-LET radiation has more damaging effects; however, these effects did not alter

the bone significantly when compared to non-irradiated control mice and thus did not negatively change bone strength.

## 5.1 Limitations

There were several limitations to the Multi-Type study and additional limitations were observed in the High-Dose study. For both studies only one follow–up time point for sacrifice. The Multi-Type study used a longer duration of 110 days to evaluate chronic effects. The High-Dose study was a shorter term study lasting only 14 days, focusing on acute affects. Using a single follow-up time could result in an inability to identify the timing of maximal bony changes. In the Multi-Type study, changes could have occurred earlier than sacrifice and the cortical bone may have recovered by the sacrifice time; however, with the addition of the High-Dose study this is unlikely to have happened within the first 14 days post-irradiation. There could have been changes in-between the 110 days from the Multi-Type and comparing the lack of cortical changes at 14 days post-irradiation from the High-Dose study. These two studies were conducted at defined times for sacrifice and critical time points that were possibly important were not observed. A time-course examination for both studies, examining periods both before and after what was examined here would give a more complete representation of the effect of radiation on both cortical and trabecular bone.

Significant changes to the cortical bone were not observed in the High-Dose study. With this higher dose and shorter time interval to sacrifice with this study, the bones likely would have started to demonstrate impending changes at the material level. The change in percent mineral composition was likely due to the inclusion of trabecular

bone (Figure 4.9) since micro-hardness testing revealed no differences between the irradiation groups and control. This suggests that several follow-up time-points and multiple doses of radiation should be evaluated to identify the full physiological effects of radiation on bones.

## 5.2 Implications

These results provide ample areas of potential study. Analysis of cortical parameters in the neck of the femur, the location of the majority of hip fractures in patients following radiotherapy, may provide further insight into the anatomic and functional consequences of irradiation. With spaceflight, a differential response in resorption is seen during micro-gravity exposure between trabecular and cortical bone (Lang et al., 2004). This results in increased fracture risk during and after missions from accelerated bone loss in reduced gravity (Lang et al., 2006), also, radiation may increase this risk. Additional studies with increased radiation dose and varying follow-up times after exposure are needed to completely describe the full physiological response of bone to conditions found in outer space.

Murine cortical bones are not vascularized in the same manner as larger animals with haversian canals systems. Cortical bone in these smaller animals might respond to radiation differently than cortical bone containing haversian canals. Tests in larger animals with haversian bone are required to evaluate the porosity and blood supply response within the cortical bone.

In comparing the two studies, shortening the follow-up time and increasing the radiation dose did not produce significant cortical bone changes. These doses were administered as a whole body dose averaged over the whole mouse. An assessment of

the actual dose to the marrow would be beneficial in calculating effect and for consistency in administering different radiation types.

Evaluating the hypothesis of ionizing density appearing greater at bone and bone marrow interface would require a computational model (Monte Carlo). The results seen in these studies and results from previous studies suggest fewer cortical bone changes, thus, less possible strength lost from the lack of cortical bone response. However, further studies are required to verify these results through basic dose range and time course analysis.

Though an LET effect was observed (significant differences between low- and high-LET radiation types), the group sizes were not large enough to demonstrate changes when compared to non-irradiated controls. Therefore, the absolute effects of radiation types on cortical bone cannot be concluded for fracture force, cortical porosity and polar moment of inertia. A power analysis using these data (difference between the means and standard deviations) would be appropriate for planning future examination of this phenomenon. It is probably best to perform the time-course examination first to explore the LET effect at the period of greatest change in cortical bone.

## 5.4 Future Directions

### 5.4.1 Clinical Experimentation

Evaluating the results and limitations of these two studies provide many directions for future research. A more clinical approach can be taken to evaluate the effects of therapeutic irradiation using a higher dose range from 1–8 Gy and a typical fractionated exposure to achieve a large cumulative dose (Bolek et al., 1996; Frassica, 2003; Nyaruba et al., 1998). The Osteoporosis Biomechanics Lab (OBL) plans to

investigate this type of dosing regimen in proposed studies delivering a 4 Gy dose administered twice per week to a cumulative exposure of 16 Gy. This would be biologically equivalent to the dose and fractionation each hip receives for treatment of pelvic tumors. Additionally, the dose placement should be evaluated.

Radiation given in a single whole body dose is less applicable to radiobiology (except for whole body irradiation preceding bone marrow transplantation), since this type of exposure is acute to the site of cancer (Bolek et al., 1996; Frassica, 2003; Nyaruba et al., 1998) . The OBL is currently studying single limb irradiation. Gamma and proton radiation are the only appropriate types for these studies because they are more controllable and widely used in medical procedures, with a preference to gamma radiation (Cosset et al., 1995).

### 5.4.2 Marrow Transplantation

Evaluating higher, potentially life threatening doses to the whole body is another avenue for future research. Detailed specifications are needed to define this area of study. Investigations would require bone marrow transplants for the mice after exposure to allow the animals to survive long enough to complete the needed analysis. Radiation exposure experimentation is applicable to bone marrow transplant patients who receive high doses of whole body radiation to eliminate functional marrow cells in preparation for transplant.

Survivability following this type of procedure requires that potential complications be evaluated and understood. Treatment for chronic lymphocytic leukemia have achieved a 74% survival rate (American Cancer Society, 2007), but these cancer patients are considered at high risk for osteoporosis because of the major age at diagnosis

is 65 years old and older (Banfi et al., 2001). It would be considered medical failure for patients to recover from bone marrow transplant then suffer a major bone fracture. This procedure could be understood using mice. The transplant procedure for mice is already developed and radiation doses are described in the literature (van Os et al., 1993; Westerhof et al., 2000). This could provide a significant opportunity to advance therapeutic options while minimizing undesirable consequences.

### 5.4.3 Spaceflight Experimentation

Future studies should also evaluate spaceflight application, in particular proton and heavy ion radiation types. This radiation exposure varies considerably in dose and dose rate (and type) compared to clinical exposures. Galactic cosmic rays are a cumulative radiation consisting primarily of protons with the presence of heavy ions (Benton and Benton, 2001; Townsend, 2005). Heavy ion (high-LET) radiation has a more damaging effect on tissue (Hamilton et al., 2006b; Ohnishi and Ohnishi, 2004). This type of radiation should be evaluated with a cumulative dose achieving 1-2 Gy over an extended time period such as 1–2 years. In evaluating a solar particle event (SPE) to a mammal, a very large range of doses can be experienced; however, primarily proton radiation would need to be evaluated, as it is the most common type of space radiation.

The major effect to be evaluated in space is the combination of radiation exposure and micro-gravity. This could be evaluated here on earth using an animal model such as hind limb suspension (Simske et al., 1991; Simske et al., 1992). This model could be combined with radiation exposure to collect data on the magnitude of damage caused by a dose of radiation to bone while experiencing micro-gravity. The differentiation of high and low-LET radiation would also need to be examined in this model. This type of

radiation is typically only seen in a space environment where high-LET has been observed to be more damaging. Radiation behind shield from high-LET types to evaluate the physiological reaction after secondary radiation particle could also be examined. More studies with an interval time course evaluation such as 1, 2, 4, 6, 10, 20, 40, etc. weeks to sacrifice are needed to evaluate the effects taking place in the interim time not examined here at 110 days post exposure, such as done in Sugimoto et al. 1991 (Sugimoto et al., 1991).

### 5.4.4 Further Cortical Analysis

Other potential research could include performing studies in the epiphyseal regions of cortical bone. This region has been shown to be more sensitive to radiation (Mitchell and Logan, 1998). This section would also have more bone turnover because of the increased activity of the trabecular bone after radiation. Specifically, the neck and proximal epiphyseal region of the femur would be of interest to study as it is a high load bearing area. The femoral neck could be mechanically tested to evaluate strength of cortical bone while controlling for changes in trabecular bone. A strain of mice with minimal trabecular bone could be chosen to evaluate these parameters without the variability of trabecular bone resorption post-irradiation. Additionally, giving the mice a bone label, such as calcein, would allow the bone formation rate to be quantified.

### 5.4.5 Anticipated Study Directions

There are several directions and experiments that would expand basic knowledge of radiation induced bone loss. This could help patients recover from radiotherapy by understanding the reaction of bone while reducing fracture risk. Further studies could

assist in developing protocols for preventative countermeasures for astronauts during longer duration spaceflight to minimize the risk of mission critical fractures. There are many types and doses of radiation to consider and increasing basic knowledge assists in preventing and mitigating physiological damage caused by exposure to radiation.

## REFERENCES


**American Cancer Society**. Cancer Facts and Figures 2006. Atlanta: American Cancer Society, 2006.

**American Cancer Society**. Cancer Facts and Figures 2007. Atlanta: American Cancer Society, 2007.

**Augat, P. and Schorlemmer, S.** (2006). The role of cortical bone and its microstructure in bone strength. *Age Ageing* **35 Suppl 2**, ii27-ii31.

**Bai, X. C., Lu, D., Bai, J., Zheng, H., Ke, Z. Y., Li, X. M. and Luo, S. Q.** (2004). Oxidative stress inhibits osteoblastic differentiation of bone cells by ERK and NF-kappaB. *Biochem Biophys Res Commun* **314**, 197-207.

**Banfi, A., Bianchi, G., Galotto, M., Cancedda, R. and Quarto, R.** (2001). Bone marrow stromal damage after chemo/radiotherapy: occurrence, consequences and possibilities of treatment. *Leuk Lymphoma* **42**, 863-70.

**Baxter, N. N., Habermann, E. B., Tepper, J. E., Durham, S. B. and Virnig, B. A.** (2005). Risk of pelvic fractures in older women following pelvic irradiation. *Jama* **294**, 2587-93.

**Benton, E. R. and Benton, E. V.** (2001). Space radiation dosimetry in low-Earth orbit and beyond. *Nucl Instrum Methods Phys Res B* **184**, 255-94.

**Bentzen, S. M.** (2006). Preventing or reducing late side effects of radiation therapy: radiobiology meets molecular pathology. *Nat Rev Cancer* **6**, 702-13.

**Bilezikian, J. P., Raisz, L. G. and Rodan, G. A.** (1996). Principles of bone biology. San Diego: Academic Press.

**Blakely, E. A.** (2000). Biological effects of cosmic radiation: deterministic and stochastic. *Health Phys* **79**, 495-506.

**Blakely, E. A., Frank Q. H. NGO, Stankely B. Curtis, and Cornelius A. Tobias.** (1984). Heavy-Ion Radiobiology: Cellular Studies. *Advances in Radiation Biology* **11**, 295-389.

**Bolek, T. W., Marcus, R. B., Jr., Mendenhall, N. P., Scarborough, M. T. and Graham-Pole, J.** (1996). Local control and functional results after twice-daily radiotherapy for Ewing's sarcoma of the extremities. *Int J Radiat Oncol Biol Phys* **35**, 687-92.

**Broz, J. J., Simske, S. J., Greenberg, A. R. and Luttges, M. W.** (1993). Effects of rehydration state on the flexural properties of whole mouse long bones. *J Biomech Eng* **115**, 447-9. **Callister, W. D.** (2007). Materials science and engineering : an introduction. New York: John Wiley & Sons.

**Coleman, R. E.** (1997). Skeletal complications of malignancy. *Cancer* **80**, 1588-94.

**Cosset, J. M., Maher, M. and Habrand, J. L.** (1995). New particles in radiotherapy: an introduction. *Radiat Environ Biophys* **34**, 37-9.

**de Gregorio, L. H., Lacativa, P. G., Melazzi, A. C. and Russo, L. A.** (2006). Glucocorticoid-induced osteoporosis. *Arq Bras Endocrinol Metabol* **50**, 793-801.

**Dong, X. N. and Guo, X. E.** (2004). The dependence of transversely isotropic elasticity of human femoral cortical bone on porosity. *J Biomech* **37**, 1281-7.

**El-Kaissi, S., Pasco, J. A., Henry, M. J., Panahi, S., Nicholson, J. G., Nicholson, G. C. and Kotowicz, M. A.** (2005). Femoral neck geometry and hip fracture risk: the Geelong osteoporosis study. *Osteoporos Int* **16**, 1299-303.

**Epelman, S. and Hamilton, D. R.** (2006). Medical mitigation strategies for acute radiation exposure during spaceflight. *Aviat Space Environ Med* **77**, 130-9.

**Findlay, D. M. and Haynes, D. R.** (2005). Mechanisms of bone loss in rheumatoid arthritis. *Mod Rheumatol* **15**, 232-40.

**Foullon, C., Andrew Holmes-Siedle, Norma Bock Crosby, Daniel Heynderickx.** (2004). Radiation Exposure and Mission Strategies for Interplanetary Manned Mission. *(REMSIM technical Note 5) Alenia Spazio Technical Note*.

**Frassica, D. A.** (2003). General principles of external beam radiation therapy for skeletal metastases. *Clin Orthop Relat Res*, S158-64.

**Goodship, A. E., Cunningham, J. L., Oganov, V., Darling, J., Miles, A. W. and Owen, G. W.** (1998). Bone loss during long term space flight is prevented by the application of a short term impulsive mechanical stimulus. *Acta Astronaut* **43**, 65-75.

**Gridley, D. S., Pecaut, M. J., Dutta-Roy, R. and Nelson, G. A.** (2002). Dose and dose rate effects of whole-body proton irradiation on leukocyte populations and lymphoid organs: part I. *Immunol Lett* **80**, 55-66.

**Gu, G., Mulari, M., Peng, Z., Hentunen, T. A. and Vaananen, H. K.** (2005). Death of osteocytes turns off the inhibition of osteoclasts and triggers local bone resorption. *Biochem Biophys Res Commun* **335**, 1095-101.

**Ha, H., Kwak, H. B., Lee, S. W., Jin, H. M., Kim, H. M., Kim, H. H. and Lee, Z. H.** (2004). Reactive oxygen species mediate RANK signaling in osteoclasts. *Exp Cell Res* **301**, 119-27.

**Hadjidakis, D. J. and Androulakis, II.** (2006). Bone remodeling. *Ann N Y Acad Sci* **1092**, 385-96.

**Hall, T. J., Schaeublin, M., Jeker, H., Fuller, K. and Chambers, T. J.** (1995). The role of reactive oxygen intermediates in osteoclastic bone resorption. *Biochem Biophys Res Commun* **207**, 280-7.

**Hamilton, S. A., Pecaut, M. J., Gridley, D. S., Travis, N. D., Bandstra, E. R., Willey, J. S., Nelson, G. and Bateman, T. A.** (2006a). A Murine Model for Bone Loss from Therapeutic and Space-Relevant Sources of Radiation. *J Appl Physiol*.

**Hamilton, S. A., Pecaut, M. J., Gridley, D. S., Travis, N. D., Bandstra, E. R., Willey, J. S., Nelson, G. A. and Bateman, T. A.** (2006b). A murine model for bone loss from therapeutic and space-relevant sources of radiation. *J Appl Physiol* **101**, 789-93.

**Hartsell, W. F., Scott, C. B., Bruner, D. W., Scarantino, C. W., Ivker, R. A., Roach, M., 3rd, Suh, J. H., Demas, W. F., Movsas, B., Petersen, I. A. et al.** (2005). Randomized trial of short- versus long-course radiotherapy for palliation of painful bone metastases. *J Natl Cancer Inst* **97**, 798-804.

**Heilbron, L., Nakamura, T., Iwata, Y., Kurosawa, T., Iwase, H. and Townsend, L. W.** (2005). Overview of secondary neutron production relevant to shielding in space. *Radiat Prot Dosimetry* **116**, 140-3.

**Holding, C. A., Findlay, D. M., Stamenkov, R., Neale, S. D., Lucas, H., Dharmapatni, A. S., Callary, S. A., Shrestha, K. R., Atkins, G. J., Howie, D. W. et al.** (2006). The correlation of RANK, RANKL and TNFalpha expression with bone loss volume and polyethylene wear debris around hip implants. *Biomaterials* **27**, 5212-9.

**Homminga, J., Weinans, H., Gowin, W., Felsenberg, D. and Huiskes, R.** (2001). Osteoporosis changes the amount of vertebral trabecular bone at risk of fracture but not the vertebral load distribution. *Spine* **26**, 1555-61.

**International Commission on Radiological Protection.** (1992). 1990 recommendations of the International Commission on Radiological Protection : user's edition. Oxford ; New York: :Published for the International Commission on Radiological Protection by Pergamon Press.

**Ito, M., Nishida, A., Koga, A., Ikeda, S., Shiraishi, A., Uetani, M., Hayashi, K. and Nakamura, T.** (2002). Contribution of trabecular and cortical components to the mechanical properties of bone and their regulating parameters. *Bone* **31**, 351-8.

**Kanis, J. A., Oden, A., Johnell, O., De Laet, C., Jonsson, B. and Oglesby, A. K.** (2003). The components of excess mortality after hip fracture. *Bone* **32**, 468-73.

**Kikuyama, A., Fukuda, K., Mori, S., Okada, M., Yamaguchi, H. and Hamanishi, C.** (2002). Hydrogen peroxide induces apoptosis of osteocytes: involvement of calcium ion and caspase activity. *Calcif Tissue Int* **71**, 243-8.

**Kinji Nishiyama, F. I., Tokurou Higashihara, Kouji Kitatani and Takahiro Kozuka.** (1992). Radiation osteoporosis — an assessment using single energy quantitative computed tomography. *European Radiology* **2**, 322-325.

**Kong, Y. Y., Feige, U., Sarosi, I., Bolon, B., Tafuri, A., Morony, S., Capparelli, C., Li, J., Elliott, R., McCabe, S. et al.** (1999). Activated T cells regulate bone loss and joint destruction in adjuvant arthritis through osteoprotegerin ligand. *Nature* **402**, 304-9.

**Lamichhane, A. P.** (2005). Osteoporosis-an update. *JNMA J Nepal Med Assoc* **44**, 60-6.

**Lang, T., LeBlanc, A., Evans, H., Lu, Y., Genant, H. and Yu, A.** (2004). Cortical and trabecular bone mineral loss from the spine and hip in long-duration spaceflight. *J Bone Miner Res* **19**, 1006-12.

**Lang, T. F., Leblanc, A. D., Evans, H. J. and Lu, Y.** (2006). Adaptation of the proximal femur to skeletal reloading after long-duration spaceflight. *J Bone Miner Res* **21**, 1224-30.

**Lorimore, S. A. and Wright, E. G.** (2003). Radiation-induced genomic instability and bystander effects: related inflammatory-type responses to radiation-induced stress and injury? A review. *Int J Radiat Biol* **79**, 15-25.

**Maeda, M., Bryant, M. H., Yamagata, M., Li, G., Earle, J. D. and Chao, E. Y.** (1988). Effects of irradiation on cortical bone and their time-related changes. A biomechanical and histomorphological study. *J Bone Joint Surg Am* **70**, 392-9.

**Marieb, E. N.** (2004). Human anatomy & physiology. New York: Pearson Education.

**Melton, L. J., 3rd.** (2000). Who has osteoporosis? A conflict between clinical and public health perspectives. *J Bone Miner Res* **15**, 2309-14.

**Mitchell, M. J. and Logan, P. M.** (1998). Radiation-induced changes in bone. *Radiographics* **18**, 1125-36; quiz 1242-3.

**MMWRMorbMortalWklyRep.** (2004). Cancer survivorship--United States, 1971-2001. *MMWR Morb Mortal Wkly Rep* **53**, 526-9.

**Mody, N., Parhami, F., Sarafian, T. A. and Demer, L. L.** (2001). Oxidative stress modulates osteoblastic differentiation of vascular and bone cells. *Free Radic Biol Med* **31**, 509-19.

**Moore, F. D.** (1992). Radiation burdens for humans on prolonged exomagnetospheric voyages. *Faseb J* **6**, 2338-43.

**Noble, B.** (2003). Bone microdamage and cell apoptosis. *Eur Cell Mater* **6**, 46-55; discusssion 55.

**Noble, B.** (2005). Microdamage and apoptosis. *Eur J Morphol* **42**, 91-8.

**Nyaruba, M. M., Yamamoto, I., Kimura, H. and Morita, R.** (1998). Bone fragility induced by X-ray irradiation in relation to cortical bone-mineral content. *Acta Radiol* **39**, 43-6.

**Oeffinger, K. C., Mertens, A. C., Sklar, C. A., Kawashima, T., Hudson, M. M., Meadows, A. T., Friedman, D. L., Marina, N., Hobbie, W., Kadan-Lottick, N. S. et al.** (2006). Chronic health conditions in adult survivors of childhood cancer. *N Engl J Med* **355**, 1572-82.

**Ohnishi, K. and Ohnishi, T.** (2004). The biological effects of space radiation during long stays in space. *Biol Sci Space* **18**, 201-5.

**Parsons, J. L. and Townsend, L. W.** (2000). Interplanetary crew dose rates for the August 1972 solar particle event. *Radiat Res* **153**, 729-33.

**Pecaut, M. J., Smith, A. L., Jones, T. A. and Gridley, D. S.** (2000). Modification of immunologic and hematologic variables by method of CO2 euthanasia. *Comp Med* **50**, 595-602.

**Pollack, L. A., Greer, G. E., Rowland, J. H., Miller, A., Doneski, D., Coughlin, S. S., Stovall, E. and Ulman, D.** (2005). Cancer survivorship: a new challenge in comprehensive cancer control. *Cancer Causes Control* **16 Suppl 1**, 51-9.

**Radiological Society of North America, A. C. o. R.** (2005). What is radiation therapy?, vol. 2006: Radiological Society of North America, Inc. .

**Rex, C. and Elsworth, C.** (1998). Pelvic insufficiency fracture with diastasis of the pubic symphysis after irradiation: a case report. *J Bone Joint Surg Br* **80**, 264-6.

**Richard E. Thacker, J.** (2004). Differentiating the Contribution of Material and Structural Properties to Changes in Bone Mechanical Strength. In *Bioengineering*, vol. Masters of Science, pp. 87. Clemson, SC: Clemson University.

**Robling, A. G., Castillo, A. B. and Turner, C. H.** (2006). Biomechanical and Molecular Regulation of Bone Remodeling. *Annu Rev Biomed Eng*.

**Rohrer, M. D., Kim, Y. and Fayos, J. V.** (1979). The effect of cobalt-60 irradiation on monkey mandibles. *Oral Surg Oral Med Oral Pathol* **48**, 424-40.

**Seeman, E. and Delmas, P. D.** (2006). Bone quality--the material and structural basis of bone strength and fragility. *N Engl J Med* **354**, 2250-61.

**Simonsen, L. C., Cucinotta, F. A., Atwell, W. and Nealy, J. E.** (1993). Temporal analysis of the October 1989 proton flare using computerized anatomical models. *Radiat Res* **133**, 1-11.

**Simonsen, L. C., Wilson, J. W., Kim, M. H. and Cucinotta, F. A.** (2000). Radiation exposure for human Mars exploration. *Health Phys* **79**, 515-25.

**Simske, S. J., Greenberg, A. R. and Luttges, M. W.** (1991). Effects of suspension-induced osteopenia on the mechanical behaviour of mouse long bones. *J Mater Sci Mater Med* **2**, 43-50.

**Simske, S. J., Guerra, K. M., Greenberg, A. R. and Luttges, M. W.** (1992). The physical and mechanical effects of suspension-induced osteopenia on mouse long bones. *J Biomech* **25**, 489-99.

**Smith, S. M., Wastney, M. E., O'Brien, K. O., Morukov, B. V., Larina, I. M., Abrams, S. A., Davis-Street, J. E., Oganov, V. and Shackelford, L. C.** (2005). Bone markers, calcium metabolism, and calcium kinetics during extended-duration space flight on the mir space station. *J Bone Miner Res* **20**, 208-18.

**Steinbeck, M. J., Kim, J. K., Trudeau, M. J., Hauschka, P. V. and Karnovsky, M. J.** (1998). Involvement of hydrogen peroxide in the differentiation of clonal HD-11EM cells into osteoclast-like cells. *J Cell Physiol* **176**, 574-87.

**Stephens, D. L., Jr., Townsend, L. W. and Hoff, J. L.** (2005). Interplanetary crew dose estimates for worst case solar particle events based on historical data for the Carrington flare of 1859. *Acta Astronaut* **56**, 969-74.

**Sugimoto, M., Takahashi, S., Toguchida, J., Kotoura, Y., Shibamoto, Y. and Yamamuro, T.** (1991). Changes in bone after high-dose irradiation. Biomechanics and histomorphology. *J Bone Joint Surg Br* **73**, 492-7.

**Sze, W. M., Shelley, M. D., Held, I., Wilt, T. J. and Mason, M. D.** (2003). Palliation of metastatic bone pain: single fraction versus multifraction radiotherapy--a systematic review of randomised trials. *Clin Oncol (R Coll Radiol)* **15**, 345-52.

**Tilton, F. E., Degioanni, J. J. and Schneider, V. S.** (1980). Long-term follow-up of Skylab bone demineralization. *Aviat Space Environ Med* **51**, 1209-13.

**Todd, P.** (2003). Space radiation health: a brief primer. *Gravit Space Biol Bull* **16**, 1-4.

**Townsend, L. W.** (2005). Implications of the space radiation environment for human exploration in deep space. *Radiat Prot Dosimetry* **115**, 44-50.

**Van der Meeren, A., Vandamme, M., Squiban, C., Gaugler, M. H. and Mouthon, M. A.** (2003). Inflammatory reaction and changes in expression of coagulation proteins on lung endothelial cells after total-body irradiation in mice. *Radiat Res* **160**, 637-46.

**van Os, R., Thames, H. D., Konings, A. W. and Down, J. D.** (1993). Radiation dose-fractionation and dose-rate relationships for long-term repopulating hemopoietic stem cells in a murine bone marrow transplant model. *Radiat Res* **136**, 118-25.

**Vico, L., Collet, P., Guignandon, A., Lafage-Proust, M. H., Thomas, T., Rehaillia, M. and Alexandre, C.** (2000). Effects of long-term microgravity exposure on cancellous and cortical weight-bearing bones of cosmonauts. *Lancet* **355**, 1607-11.

**Viguet-Carrin, S., Garnero, P. and Delmas, P. D.** (2006). The role of collagen in bone strength. *Osteoporos Int* **17**, 319-36.

**Westerhof, G. R., Ploemacher, R. E., Boudewijn, A., Blokland, I., Dillingh, J. H., McGown, A. T., Hadfield, J. A., Dawson, M. J. and Down, J. D.** (2000). Comparison of different busulfan analogues for depletion of hematopoietic stem cells and promotion of donor-type chimerism in murine bone marrow transplant recipients. *Cancer Res* **60**, 5470-8.

**Willey, J. S., Gridley, D. S., M.J., P., Norrdin, R. W., C.L., S. and T.A., B.** (Submitted 2007). A 7 Gray Dose of Gamma-Radiation Causes a Profound and Rapid Loss of Trabecular Bone in Mice. *Journal of Bone and Mineral Metabolism*.